c-Jun/p38MAPK/ASIC3 pathways specifically activated by nerve growth factor through TrkA are crucial for mechanical allodynia development

Tanguy Chaumette, Lauriane Delay, Julie Barbier, Ludivine Boudieu, Youssef Aissouni, Mathieu Meleine, Amandine Lashermes, Wassim Legha, Sophie Antraigue, Frédéric Antonio Carvalho, et al.

PAIN

c-Jun/p38MAPK/ASIC3 pathways specifically activated by NGF through TrkA is crucial for mechanical allodynia development

--Manuscript Draft--

Manuscript Number:	PAIN-D-19-00901R2
Full Title:	c-Jun/p38MAPK/ASIC3 pathways specifically activated by NGF through TrkA is crucial for mechanical allodynia development
Article Type:	Research Paper
Keywords:	NGF, TrkA, mechanical allodynia, ASIC3, p38MAPK
Corresponding Author:	Fabien Marchand, PhD Inserm, U 1107, Clermont Université, Université d'Auvergne Clermont-Ferrand, FRANCE
Corresponding Author Secondary Information:	
Corresponding Author's Institution:	Inserm, U 1107, Clermont Université, Université d'Auvergne
Corresponding Author's Secondary Institution:	
First Author:	Tanguy Chaumette, PhD
First Author Secondary Information:	
Order of Authors:	Tanguy Chaumette, PhD
	Lauriane Delay, PhD
	Julie Barbier, Technician
	Boudieu Ludivine, PhD
	Youssef Aissouni, PhD
	Mathieu Meleine, PhD
	Lashermes Amandine, PhD
	Wassim Legha, PhD
	Sophie Antraigue, student
	Frederic Carvalho, PhD
	Alain Eschalier, PhD, MD, PharmD
	Denis Ardid, PhD
	Aziz Moqrich, PhD
	Fabien Marchand, PhD
Additional Information:	
Question	**Response**
Have you posted this manuscript on a preprint server (e.g., arXiv.org, BioXriv, PeerJ Preprints)?	No

Unité Mixte de Recherche
Inserm / UCA 1107
NEURO-DOL
Directeur : Pr. Denis Ardid

Clermont-Ferrand, 7th of January 2020

Dear Editor,

Please find enclosed our revised manuscript entitled *"c-Jun/p38MAPK/ASIC3 pathways specifically activated by NGF through TrkA is crucial for mechanical allodynia development*" which we would like considered following revision by Pain.

As listed in our reply to the section editor and referees comments, we have answered all questions and have made changes accordingly in the manuscript.

We would like to thanks the section editor and reviewers for their useful comments and hope that they will find this revised version of our manuscript suitable for publication in Pain.

Thank you for your consideration.

Yours sincerely

UMR1107 Inserm/UCA
PHARMACOLOGIE FONDAMENTALE ET CLINIQUE DE LA DOULEUR
FACULTE DE MEDECINE
28, Place Henri Dunant, B.P. 38 - 63001 CLERMONT-FERRAND Cedex 1(France)
Téléphone (33) 4 73 17 82 30 Télécopie (33) 4 73 27 46 21

We are very grateful for the constructive comments of the reviewers and section editor which have improved the quality of our manuscript. The manuscript has been modified according to the section editor comment. We look forward to hearing back from you on this revised submission. A response to the section editor comment is below in blue. Changes made in the manuscript appear in red.

Section Editor: I agree that the reviewers have addressed most of the previous comments, but I still think there is an issue that is not resolved. The authors state in the discussion that p38 and c-JUN are "essential" for NGF-induced allodynia, but they have not really tested this. No interventions were done for c-Jun, although others have done this for p38 inhibitors (e.g. the Ji lab). My major issue here is that ERK and mTOR are also very well known to be activated by mTOR and the authors seem to have ruled these out based on their PCR experiment. However, PCR is not really appropriate here because it does not matter if the RNA changes, what matters is the kinase activity. I think this was a point of the second review, who was unfortunately not available to re-review the paper. I do agree that this is a clever model to clearly delineate the signaling pathways that are necessary for NGF-induced mechanical allodynia, but I just am not sure that the authors can really conclude that they have discovered an "essential" pathway based on their experimental approach.

We agree that ERK and mTOR could be also activated by NGF in TrkAC mice and that PCR is definitely not the best approach to assess kinases activities. However, given the number of kinases that needed to be tested, it appeared to us at that time that it was the best approach. Here, we only privileged p38MAPK and c-Jun as important players in NGF induced mechanical allodynia but not allodynia/hyperalgesia in general. Actually, we even think that ERK and probably mTOR are crucial for NGF induced thermal hyperalgesia since ERK has been shown to modulate TRPV1 activity and mediated NGF induced heat hyperalgesia (Zhuang et al., 2004). Importantly, we also showed previously that levels of pERK were significantly increased in TrkAC DRG neurons in culture 5 and 15 min after NGF stimulation compared to non-stimulated TrkAC neurons. Moreover, ERK activation was similar between TrkAC and wild type neurons, at least, 5 min after NGF stimulation (see Figure S2, Gorokhova et al, 2014). Thus, it seems that the activation of this pathway is comparable between TrkAC and WT. Since we did not test this hypothesis here and, it was a bit beyond the scope of the discussion, we did not discussed it.

Nonetheless, the wording “essential” has been down toned and replaced by “probably very important” in the discussion.

Finally, we agree with the section editor that we did not test directly p38 inhibition as in Ji paper for example. However as stated in our first reply, the inhibition of p38MAPK in WT animal specifically in the DRG and even in TrkA positive neurones will be experimentally very challenging. Pharmacologically, intrathecal administration of a p38MAPK specific inhibitor such as SB203580 as done in Ji paper, will inhibit p38MAPK in the DRG but we also think at the spinal level especially in microglia. However, p38 MAPK inhibition in the spinal cord inhibited both mechanical and thermal hypersensitivities following peripheral inflammation (Tan et al 2010; Svensson et al., 2003). Administration of the p38MAPK inhibitor within mice DRG is a technic that we have never experienced before and has been done in very few studies. Genetically, only $p38\alpha^{loxP/loxP}$ mice are available and crossing these mice with an Adv-Cre or Nav 1.8-Cre mice for example will only ablate the p38αMAPK isoform and not all the p38MAPK different isoforms. Finally, a virus approach could be possible but will require a lot of preliminary experiments to be fully validated.

Phosphatidylinositol 3-kinase activates ERK in primary sensory neurons and mediates inflammatory heat hyperalgesia through TRPV1 sensitization. Zhuang ZY, Xu H, Clapham DE, Ji RR. J Neurosci. 2004 Sep 22;24(38):8300-9

Activation of Src family kinases in spinal microglia contributes to formalin-induced persistent pain state through p38 pathway. Tan YH, Li K, Chen XY, Cao Y, Light AR, Fu KY. J Pain. 2012; 13(10):1008-15.

Activation of p38 mitogen-activated protein kinase in spinal microglia is a critical link in inflammation-induced spinal pain processing. Svensson CI, Marsala M, Westerlund A, Calcutt NA, Campana WM, Freshwater JD, Catalano R, Feng Y, Protter AA, Scott B, Yaksh TL J Neurochem. 2003;86(6):1534-44.

Reviewer #1: The authors have made significant efforts in addressing my concerns. I have no further issues.

We would like to thanks again the reviewer 1 for his useful comments

Supplementary figures need to be cited in consecutive order. Please revise accordingly.

This has been revised accordingly

Abstract

Mechanical allodynia is a cardinal sign of several inflammatory pain disorders where Nerve Growth Factor, a prototypic neurotrophin, plays a crucial role by binding to TrkA receptors. Here, we took the advantage of our generated knock-in mouse model expressing a chimeric TrkA/TrkC receptor that seems to not specifically develop mechanical allodynia following inflammation, to identify the TrkA downstream pathways involved in this phenomenon. We confirmed and extended that disrupting TrkA specific pathways leads to a specific deficit in mechanical hypersensitivity development following somatic (systemic NGF administration and paw incision) and to a lesser extent, visceral injuries. Despite a deficit in thin, mainly peptidergic, fibres innervation in TrkAC mice, thermal hyperalgesia development was not different from WT mice. Inflammatory reaction (oedema, IL-6 content), pain behaviours following intraplantar capsaicin as well as TRPV1 calcium imaging response of DRG neurons were similar between TrkAC and WT mice. This deficiency in mechanical allodynia development in TrkAC mice is likely due to the alteration of the expression of different TrkA transduction pathways (*i.e*. Akt, p38 MAPK and c-Jun) especially p38 MAPK, in the DRG cell bodies, ultimately leading to an alteration of at least, ASIC3 channel overexpression, known to participate in nociceptor mechanosensory function.

c-Jun/p38MAPK/ASIC3 pathways specifically activated by NGF through TrkA is crucial for mechanical allodynia development

Tanguy Chaumette [1*], Lauriane Delay [1*], Julie Barbier [1], Ludivine Boudieu [1], Youssef Aissouni [1], Mathieu Meleine[1], Amandine Lashermes [1], Wassim Legha [1], Sophie Antraigue [1], Frederic Antonio Carvalho [1], Alain Eschalier [1], Denis Ardid [1], Aziz Moqrich [2], Fabien Marchand [1†]

1. Université Clermont Auvergne, Inserm U1107 NEURO-DOL, Pharmacologie fondamentale et clinique de la douleur, F-63000 Clermont-Ferrand, France.

2. Institut de Biologie du Développement de Marseille Luminy, UMR 6216 CNRS-Université de la Méditerranée, Campus de Luminy case 907, 13288 Marseille Cedex 09, France.

† **Corresponding author:** Fabien Marchand. Université Clermont Auvergne, Inserm U1107 NEURO-DOL, Pharmacologie fondamentale et clinique de la douleur, 28 place Henri Dunant, BP 38, 63000 Clermont-Ferrand Cedex 01, France.

Tel: +33 473178231; Fax: +33 473274621. Email address: fabien.marchand@uca.fr

*These authors contributed equally to this work

Total number of pages: 44

Number of figures: 6

Number of supplementary figures: 3

Number of tables: 3

c-Jun/p38MAPK/ASIC3 pathways specifically activated by NGF through TrkA is crucial for mechanical allodynia development

Chaumette T[1*], Delay L[1*], Barbier J[1], Boudieu L[1], Aissouni Y[1], Meleine M[1], Lashermes A[1], Legha W[1], Antraigue S[1], Carvalho F[1], Eschalier A[1], Ardid D[1], Moqrich A[2], Marchand F[1†]

1. Université Clermont Auvergne, Inserm U1107 NEURO-DOL, Pharmacologie fondamentale et clinique de la douleur, F-63000 Clermont-Ferrand, France.

2. Institut de Biologie du Développement de Marseille Luminy, UMR 6216 CNRS-Université de la Méditerranée, Campus de Luminy case 907, 13288 Marseille Cedex 09, France.

† **Corresponding author:** Fabien Marchand. Université Clermont Auvergne, Inserm U1107 NEURO-DOL, Pharmacologie fondamentale et clinique de la douleur, 28 place Henri Dunant, BP 38, 63000 Clermont-Ferrand Cedex 01, France.

Tel: +33 473178231; Fax: +33 473274621. Email address: fabien.marchand@uca.fr

*These authors contributed equally to this work

Total number of pages: 44

Number of figures: 6

Number of supplementary figures: 3

Number of tables: 3

Abstract

Mechanical allodynia is a cardinal sign of several inflammatory pain disorders where Nerve Growth Factor, a prototypic neurotrophin, plays a crucial role by binding to TrkA receptors. Here, we took the advantage of our generated knock-in mouse model expressing a chimeric TrkA/TrkC receptor that seems to not specifically develop mechanical allodynia following inflammation, to identify the TrkA downstream pathways involved in this phenomenon. We confirmed and extended that disrupting TrkA specific pathways leads to a specific deficit in mechanical hypersensitivity development following somatic (systemic NGF administration and paw incision) and to a lesser extent, visceral injuries. Despite a deficit in thin, mainly peptidergic, fibres innervation in TrkAC mice, thermal hyperalgesia development was not different from WT mice. Inflammatory reaction (oedema, IL-6 content), pain behaviours following intraplantar capsaicin as well as TRPV1 calcium imaging response of DRG neurons were similar between TrkAC and WT mice. This deficiency in mechanical allodynia development in TrkAC mice is likely due to the alteration of the expression of different TrkA transduction pathways (*i.e*. Akt, p38 MAPK and c-Jun) especially p38 MAPK, in the DRG cell bodies, ultimately leading to an alteration of at least, ASIC3 channel overexpression, known to participate in nociceptor mechanosensory function.

Keywords: NGF, TrkA, ASIC3, mechanical allodynia, p38MAPK

Introduction

Mechanical allodynia is the hallmark of several types of chronic pain disorders. Following tissue injuries or chemical insults, several substances are released within the local tissue environment, ultimately changing the excitability of nociceptors and leading to different painful symptoms including mechanical allodynia. One of the most important substance is the nerve growth factor (NGF), a prototypic neurotrophin, which is critical for the development and maintenance of autonomic and sensory neurons, including nociceptors, in the developing nervous system [9,25]. In the adult, systemic or local administration of NGF in rodents and human results in profound and long lasting heat and mechanical hypersensitivity by binding mainly to TrkA receptors [40]. By contrast, blocking NGF effects by different strategies prevents the sensitization of nociceptors in several pain models (for review [9,25,32,34]). Following TrkA binding, NGF activates various intracellular pathways such as PLCγ/PKC pathway, phosphatidylinositol 3-kinase pathway (PI_3-K) [54], mitogen-activated protein kinase kinase/mitogen-activated protein kinase pathways (MAPKK/MAPK) including Erks, JNKs, and p38 MAPK [23,33,39,53]. Several of these downstream pathways such as MEK/ERK, PI3K, PKMzeta and PLCγ have been proposed as second messengers of NGF induced mechanical hypersensitivity [21,28]. However, the role of NGF in both mechanical allodynia and thermal hyperalgesia has not been systematically assessed in these studies, and the injection of specific inhibitors of these pathways or NGF has been mostly performed into the hindpaw. Thus, the second messengers signalling pathways by which NGF acts specifically to sensitize nociceptors to mechanical stimulation and up regulates mechanically activated currents, still remain elusive. Therefore, it is crucial to better understand the precise mechanisms by which NGF leads to mechanical allodynia since anti-NGF drugs have the potential to make a major impact on chronic pain treatment in the near future but are associated with potential adverse events.

Interestingly, we have previously shown that our generated knock-in mouse expressing a chimeric TrkAC receptor, formed by the extracellular part of TrkA and the functional transmembrane and intracellular parts of TrkC, the receptor of neurotrophin 3, seems to exhibit a specific deficit in mechanical allodynia but not thermal hyperalgesia following intraplantar CFA injection [16]. Importantly, while nociceptors survival and maturation are normal in the TrkAC adult mice, they present a reduction in peripheral, mostly peptidergic fibers, in the skin. However, the expression of both mechanosensory TrkB positive fibers and Ret in large diameter neurons, representing the ‘‘early Ret’’ population of rapidly adapting mechanoreceptors, remained unchanged in TrkAC mice [16]. The aim of our study was to use this particular deficit of mechanical allodynia development in TrkAC mice to investigate and better understand the role of NGF/TrkA-activated intracellular pathways in this phenomenon following somatic and visceral injuries.

Methods

Animals

TrkAC knock-in animals and WT-littermates from C57BL/6J background were bred in our animal facility and housed in a controlled room with a 12-hour light/dark cycle, with free access to food and water. All procedures were approved by the local ethical committee (Comité Régional d'éthique en matière d'expérimentation animale Auvergne (CEMEA-Auvergne)) and in accordance with European Communities Council Directive for the care of laboratory animals (86/609/EEC). Experiments followed guidelines of the International Association for the Study of Pain and ARRIVE [41,57].

Only male TrkAC and WT-littermates (10-12 weeks old) have been used for somatic pain models (systemic NGF injection induced pain and plantar incisional pain model) except for intraplantar capsaicin where both female/male TrkAC and WT-littermates were used. Only female TrkAC and WT-littermates (10-12 weeks old) have been used for the visceral pain model induced by cyclophosphamide administration and both male and female for colorectal distension.

All experiments were performed in a randomized block design to control variability and avoid any unspecific effects across the experiment. The experimenter was blind regarding the genotype (WT or TrkAC mice) and treatment administered (*i.e.*, NGF, surgery or cyclophosphamide).

Pain models

Systemic NGF injection induced pain

Systemic administration of NGF has been shown to induce thermal and long lasting mechanical hypersensitivity [22,26]. Briefly, NGF (2.5S, Sigma Aldrich) was administered by subcutaneous route (0.1mL/10g) at the dose of 1mg/kg. Paw mechanical and thermal thresholds (see below) were assessed 24h before NGF injection and at 4h,

6h, 24h and 1h, 6h, 24h following NGF injection, respectively. n=8 animals in each group (WT + NGF and TrkAC + NGF).

Plantar incisional pain model

The post-operative pain model following plantar incision was used [4]. Animals were anesthetized with 2-2.5% isoflurane and the skin of the operated paw was cleaned with povidone iodine 10% (Merck) and placed in the hole of a sterile drape. The glabrous skin and fascia of the left hind paw were incised longitudinally, starting 0.2 cm from the proximal edge of the heel, and the underlying flexor muscle was elevated, divided, and retracted. After haemostasis, the skin overlying the muscle was closed with two sutures of 5.0 polyamide monofilament (Ethicon, Somerville, NJ, USA). Animals were allowed to recover from anaesthesia. n=13-15 animals in each group (WT incision and TrkAC incision).

Cyclophosphamide induced-cystitis

Cystitis was induced by a single intraperitoneal injection of cyclophosphamide (CYP, Leancare Ltd, UK). Animals received either cyclophosphamide (150 mg/kg in 0.9% NaCl) or vehicle (0.9% NaCl) [24]. n=13-15 animals in each group (WT + saline, TrkAC + saline, WT + CYP and TrkAC + CYP).

Capsaicin-induced spontaneous behaviour

Following acclimation in individual acrylic glass boxes, mice were injected with a single intraplantar administration of capsaicin in the hindpaw (1.5µg/20µL/mice, Sigma-Aldrich) as described previously [37,44]. Spontaneous nocifensive behaviours (*i.e.* licking, biting, lifting, and flinching) of the injected paw were measured for 5 minutes following capsaicin administration. n=6-7 animals in each group (WT + capsaicin, TrkAC + capsaicin).

Behavioural pain tests

Assessment of paw mechanical allodynia in systemic NGF and the plantar incisional pain models

Paw mechanical sensitivity in NGF and plantar incisional pain models was assessed using von Frey's hairs based on the up-down method developed by Chaplan [7] and modified by Dixon [14]. The von Frey's hairs used were: 0.02, 0.04, 0.07, 0.16, 0.4, 0.6, 1, 1.4g. Animals were acclimatised for at least 1h in individual clear acrylic cubicles (22 × 16.5 × 14 cm) placed on the top of an elevated wire mesh. The filaments were applied on the hind paw with a 5 min interval between stimuli. Quick withdrawal or licking of the paw to the stimulus was considered a positive response. Threshold values were derived according to the method described by Chaplan [7]. If the animal showed no response to the highest von Frey hair, the von Frey threshold of 1.4 g was assigned. If the animal showed response to all von Frey hairs, the von Frey threshold of 0.02 g was assigned. The 50% paw mechanical threshold was evaluated before and 2h, 24h and 48h following paw incision, and before and 4h, 6h, 24h following systemic NGF administration.

Assessment of referred mechanical allodynia in the cystitis model

Abdominal mechanical sensitivity in the CYP induced cystitis model was assessed with von Frey's hairs using the up-down method developed by Chaplan [7] and modified by Dixon [14], von Frey's hairs used were similar as those used for the paw. Briefly, animals were acclimatised for 1h on an elevated wire mesh in individual clear acrylic cubicles (22 × 16.5 × 14 cm) placed on the top of an elevated wire mesh. Abdominal stimulation was then realised starting with the middle 0.16g hair and followed by up and down stimulation. Quick withdrawal/licking of the abdomen or biting of the hair to the stimulus was considered a positive response. The 50% abdominal mechanical threshold was determined before and 4h, 24h and 48h following CYP administration.

Assessment of thermal hyperalgesia in systemic NGF and the plantar incisional pain models

Thermal hyperalgesia was assessed in the systemic NGF and plantar incisional pain models using the plantar test as previously described by [18]. Each animal was placed in clear acrylic cubicles (22 × 16.5 × 14 cm) on top of a glass floor in a temperature controlled room (~22°C) and allowed to acclimatise for 1h before testing. The hindpaw was stimulated with a radiant heat source (Bioseb) placed under the glass floor. Withdrawal latencies were averaged over three consecutive tests, at least 10 min apart, in response to the thermal challenge from a calibrated radiant light source (output of 190 mW/cm2). A cut-off of 20s was imposed to prevent any tissue damage. Thermal threshold was assessed 24h before and 2h, 24h and 48h following paw incision and before, 1h, 6h and 24h following NGF administration.

IL-6 ELISA

At two time points of the behavioural pain experiments (*i.e.,* 2h and 48h following plantar incision and 4h and 48h following CYP administration), n=4-5 animals in each group at each time point were terminally anaesthetised using pentobarbitone. The incised paw skin and the bladder for the incisional pain model and the cystitis pain model, respectively, were quickly dissected out and snap frozen in liquid nitrogen. Tissue samples were subsequently homogenized in lysis buffer (137mM NaCl, 20mM TrisHCl, 1% NP40, 10% glycerol, 1mM PMSF, 10µg/mL aprotinin, 1µg/mL leupeptin, 0.5mM sodium vanadate) using a glass homogenizer. Homogenates were then centrifuged at 14 000g for 10min at 4°C and supernatants were collected. Whole cell lysates were next titrated to determine their protein concentrations using a BCA Protein Assay kit (Pierce, UK).

Interleukin-6 (IL-6) content was measured using DuoSet Elisa (#DY406, R&D system, Minneapolis, USA). IL-6 content was determined using a quantitative sandwich

enzyme immunoassay technique according to the manufacturer's guidelines. Samples were processed in triplicate and values were calculated from the standard sample curve in the linear range. IL-6 contents in the paw skin and bladder were assessed 2h and 48h and 4h and 48h, respectively, after injuries.

Calcium Imaging

DRG neurons primary culture

Dorsal root ganglia from 12 weeks old TrkAC knock-in and WT littermate mice (n=1 per genotype) were quickly collected in ice-cold Hanks' balanced salt solution (HBSS) and incubated 45min at 37°C in 5% CO_2 in a digestion enzyme mix containing: Collagenase type 3 (5mg/mL), Dispase (10mg/mL), Glucose 10mM and HEPES 5mM in Ca^{2+} and Mg^2 free HBSS. After dissociation, DRGs were transferred in a tube containing Dulbecco's modified Eagle's medium (DMEM) supplemented with heat-inactivated Fetal Bovine Serum 10%, L-Glutamine 2mM, Minimum Essential Vitamins solution 1%, Penicillin/Streptomycin solution 1%, Sodium Pyruvate 1mM and Non-essential amino acids solution 1%. Ganglia were gently triturated using fire-polished glass Pasteur pipettes. After centrifugation, cells were resuspended in supplemented DMEM and plated on poly-L-lysine and laminin-coated glass coverslips. Neurons were kept at 37°C in 5% CO_2 and used for calcium imaging experiments within 2 days following culture.

Imaging

DRG neurons were washed twice with DMEM and incubated for 45min at 37°C under gentle shaking in DMEM containing Fura-2 AM 4µM and Pluronic Acid 0.04%. DRG neurons were then washed twice in Krebs-Ringer solution containing NaCl 140mM, KCl 3mM, MgCl2 1mM, CaCl2 2mM, D-Glucose 10mM and HEPES 10mM with pH adjusted at 7.4 and osmolarity at 300mOsm. Coverslips were mounted on the recording chamber and placed on the platform of an inverted microscope (Zeiss). Intracellular calcium

changes were recorded at x10 magnification by alternatively illuminating cells with 340nm and 380nm LED light sources with an exposure time of 200ms for each wavelength. Fluorescence emission at 510nm was acquired every 2 seconds using a CCD camera and recorded using MetaFluor® software. The ratio of F340/F380 fluorescence intensity was calculated for each cell and averaged for each conditions.

The calcium imaging has been done on 4 separate dishes with 2 dishes for each genotype (*i.e.,* WT and TrkAC). During experiments neurons were continuously superfused with Krebs-Ringer solution. Cells were stimulated 5 times with capsaicin (100nM in Krebs-Ringer solution) for 15s with a 4min interval between each stimulation. At the end of the experiment all excitable cells were identified by the application of high-KCl Krebs-Ringer solution (NaCl 93mM, KCl 50mM, MgCl2 1mM, CaCl2 2mM, D-Glucose 10mM and HEPES 10mM with pH adjusted at 7.4 and osmolarity at 300mOsm) for 1min. For peak intensity calculation, the ratio value just prior to the start of the stimulus was subtracted from the maximum ratio value within the 80 seconds following capsaicin application or within 60 seconds after KCl application (50mM). Only cells displaying an increase of at least 15% of their peak intensity in response to KCl were included for analysis. Among them, cells were considered as positive to capsaicin if their peak intensity was increased by at least 15% upon the first capsaicin exposure. In total, 257 cells for the WT and 377 cells for the TrkAC conditions have been kept for analysis.

Quantitative PCR of NGF/TrkA signalling pathways in lumbar DRGs following plantar incision or cystitis in WT and TrkAC mice

To investigate changes in the NGF/TrkA signalling pathways in the plantar incision and cystitis models, we performed quantitative PCR (q-PCR) on DRGs 48h after incision or CYP administration. WT and TrkAC mice (n=3-5 per group for the paw incision model and n=4-6 per group for the CYP model) were terminally anaesthetised using

pentobarbitone and ipsilateral and contralateral lumbar DRGs (L4, L5, L6 and L6, S1 for the plantar incision and cystitis models, respectively) were quickly dissected out, snap frozen in liquid nitrogen and stored at −80 °C until use. Total RNA was extracted using Quick-RNA_MicroPrep kit (ZymoResearch, Epigenetics, USA) according to the manufacturer's protocol. The concentration of RNA was quantified using Take3 nucleic acid quantification plate (Epoch, BioTek, USA). Equal amounts of RNA from each sample were reverse transcribed in a volume of 20µl to produce cDNA using High Capacity cDNA Reverse Transcription Kit (Applied Biosystems, USA) following the manufacturer's recommendation.

SYBR Green-based detection was carried out on a real-time PCR instrument (RealPlex, Eppendorf, GmBH) with thermal cycler conditions of: 95 °C for 30s, followed by 45 cycles (95 °C for 10s, 59 °C for 15s and 72°C for 15s). In each experiment, samples were assayed in triplicate. Data were analysed using the threshold cycle (Ct) relative quantification method. Relative quantities (RQ) were determined using the equation: $RQ = 2^{-\Delta\Delta Ct}$. β-Actin was used as housekeeping gene. Forward and reverse primers used are presented in Table 1.

Western immunoblotting

Forty eight hours after paw incision, WT and TrkAC animals (n=10 for each genotype) were terminally anaesthetized with pentobarbitone, ipsilateral and contralateral L4-L5-L6 DRGs were dissected out and snap frozen in liquid nitrogen. The ipsilateral or contralateral DRGs of two animals (*i.e.* 6 DRGs in total for each side) of the same genotype were pooled together and homogenized in RIPA (RadioImmunoPrecipitation Assay) buffer (50 mM Tris HCl pH 7.5, 150 mM NaCl, 1 mM EDTA, 1% NP-40, 0.1% SDS + 0.5% Deoxycholic acid containing complete protease inhibitor cocktail) using a glass homogenizer. Homogenates were then centrifuged at 14 000g for 10min at 4°C and

supernatants were collected. DRGs whole cell lysates were next titrated to determine their protein concentrations using a BCA Protein Assay kit (Pierce, UK).

For Western immunoblotting, Laemmli loading buffer was added to the samples and heated at 70°C for 30 min. The DRG homogenates (40µg protein) were separated using 4-20% SDS-PAGE pre-cast polyacrylamide gels. The separated proteins were then transferred to PVDF membranes using Trans-Blot Turbo blotting system (Bio-Rad, USA). All membrane incubations were performed on a rotating plate. Washes were done in TBS-T (50 mM Tris-HCl and 6 mM NaCl containing 0.1% Tween 20). Blocking of unspecific binding sites was done by incubating the membranes in 5% non-fat dry milk in TBS-T or 5% BSA in TBS-T when is indicated for 1 hour at room temperature. The membranes were then incubated with the primary antibodies against the unphosphorylated form of Akt or p38MAPK (see below, Cell Signalling Technology) diluted in 5% non-fat milk in TBS-T or 5% BSA in TBS-T overnight at 4°C. After washing, the membranes were probed with appropriate Horseradish peroxidase conjugated secondary antibody diluted (1:10,000) with 5% non-fat dry milk in TBS-T or 5% BSA in TBS-T for 1 hour at room temperature. Following this first incubation and revelation, the blots were stripped twice with stripping buffer (0.2 M Glycine, 0.1% SDS, 1% Tween-20; pH 2.0), blocked and reprobed with the primary antibodies against the phosphorylated form of Akt or p38MAPK (see below).

Antibodies against phospho-p38 MAPK (Thr180/Tyr182, 1:2000; catalog #9216) and p38 MAPK (1:1000; catalog #8690) were diluted in 5% BSA in TBS-T. Antibodies against phospho-Akt (ser473, 1:1000; catalog #9271) and total Akt (1:1000; catalog #9272) were diluted in 5% non-fat milk in TBS-T. β-actin (1:5000; Sigma) was used as loading control.

The immunoreactive bands were quantified by densitometry analysis using Bio-Rad imaging software (Chemidoc). Phospho bands of p-Akt and p-p38 MAPK were

normalized relative to total Akt and p38 MAPK, respectively, with all bands already normalized to β-actin. Results are expressed as the mean ± SEM of expression levels of contralateral and ipsilateral DRGs for each group (both ipsilateral and contralateral protein samples were run on the same gel).

Retrograde labelling of bladder DRG neurons

A retrograde labelling of DRG neurons specifically innervating the bladder for subsequent immunochemistry was realised one week before saline or CYP administration. Animals were anaesthetized with 2% isoflurane. Following a laparotomy, the bladder was carefully exposed. Eight µL of fluorogold (#39286; Hydroxystilbamidine bis (methanesulfonate), Sigma Aldrich) were very slowly administered in four different injection sites (2µL per site) in the dorsal bladder wall. Great care was taken to not go through the bladder wall. For each injection, the needle was left in the bladder wall for at least 1min to avoid leaking. The injection sites were then wiped and the bladder thoroughly washed with NaCl 0.9%. The bladder was then repositioned in the abdominal cavity and the abdominal muscles wound closed with 5.0 sutures (Ethicon, Somerville, NJ, USA). Wound skin was closed with 3.0 sutures (Ethicon, Somerville, NJ, USA).

Immunohistochemistry

DRG immunohistochemistry

At the end of the behavioural experiments (*i.e.* 48h after plantar incision or following CYP or saline administration), n=5 animals in each group and genotype (*i.e.* WT and TrkAC) were terminally anaesthetised using pentobarbitone and quickly perfused transcardially with saline followed by 4% paraformaldehyde (PFA). After perfusion, ipsilateral L4-L5-L6 DRGs for the incisional pain model and L6 DRGs and the bladder for the CYP model were excised, post-fixed 4h for DRGs and 12h for the bladder in the same

perfusion fixative, cryoprotected in 30% sucrose in 0.1 M phosphate buffer (PB) for at least 48h at 4°C, and then frozen in tissue freezing medium (O.C.T). Transverse DRG sections (10µm) were cut on cryostat, dried for 30 min at room temperature and then stored at -20°C before staining.

DRG sections were stained as follow: after 3 washes in PBS containing 0.2% triton X-100 and 1% BSA, sections were incubated overnight at room temperature in a humid chamber with primary antibodies (*i.e.,* ASIC3, CGRP, TrkA) diluted as indicated in **Table 2** in antibody diluent (#S2022; Dako). Following 5 washes 5 min each in PBS, sections were then incubated with the appropriate secondary antibodies (**Table 2**) diluted in the same antibody diluent for 2h at room temperature. Sections were then washed 3 times in PBS and cover-slipped with fluorescent mounting medium (Dako).

Sections were visualised under a Nikon Eclipse Ni-E fluorescent microscope run with Nikon analysis software (NiS element). DRG neurons counts were done by a blind experimenter on L4-L5-L6 DRGs for the post incisional pain model and L6 DRG for the cystitis model (4-6 sections for each animal, n=5 per group and conditions (i.e. paw incision and CYP administration)).

Bladder immunohistochemistry

Bladder cryostat cut sections (20µm) from the different groups were stained with the primary antibody against CGRP (rabbit anti-CGRP, 1:1000, **Table 2**), as described above for DRG sections, to assess peptidergic innervation. Bladder sections were visualised under a Nikon Eclipse Ni-E fluorescent microscope run with Nikon analysis software (NiS element). The percentage of CGRP staining was automatically quantified in a ROI including all the bladder area (n=5-6) for each animal in each group (n=4-5 per group).

Statistics

Results are expressed as mean ± standard error to mean (S.E.M). A one-way analysis of variance (ANOVA) was used to compare more than two groups, followed by Tukey test for multiple comparisons with repeated measures when appropriate. When treatment and time were compared, a two-way ANOVA was used. When the F value was significant, this was followed by Tukey test for multiple comparisons. For calcium imaging a two-way ANOVA followed by Holm-Sidak multiple comparison test was used. Neuronal DRG counting and q-PCR results have been analysed using a non-parametric Mann-Whitney test. Results were analysed with GraphPad prism 6 software (GraphPad Prism version 6.00 for Windows, GraphPad Software, La Jolla California USA). In all cases, the significance level was set at $p<0.05$.

Results

Specific lack of mechanical allodynia development in TrkAC mice following somatic and to a lesser extent visceral injuries.

To confirm that the lack of mechanical allodynia development previously observed in TrkAC animals following intraplantar CFA is directly mediated by NGF activation of TrkA receptors, NGF was delivered by subcutaneous route (1mg/kg) in both WT and TrkAC mice. Before NGF injection, 50% mechanical thresholds (*i.e.,* baseline) were not different between both genotypes (**Fig. 1A**). As expected, WT mice developed both mechanical allodynia from 4h to 24h ($p \leq 0.0001$ for each time point) and thermal hyperalgesia from 1h to 6h ($p=0.002$ and $p=0.0009$, respectively), following NGF administration compared to baseline (**Fig. 1A&B**). By contrast, TrkAC animals did not exhibit mechanical allodynia at any time point compared to WT ($p=0.003$, $p=0.001$ and $p=0.034$ at 4, 6 and 24h respectively). They only displayed significant thermal hyperalgesia from 1h to 6h ($p=0.009$ and $p=0.002$ respectively), similarly to WT (**Fig. 1A&B**).

We also assessed pain behaviours in the plantar incisional model. Before plantar incision, 50% mechanical thresholds (*i.e.,* baseline) were not different between WT and TrkAC mice (**Fig. 1C**). Following plantar incision, WT animals exhibited mechanical allodynia from 2h to 48h ($p=0.008$, $p=0.003$ and $p=0.006$ at 2, 24 and 48h, respectively), characterized by a significant decrease of 50% mechanical thresholds compared to baseline (**Fig. 1C**). By contrast, TrkAC mice did not develop mechanical allodynia throughout the whole study with 50% mechanical thresholds similar to their baseline values but different from WT mice ($p=0.006$, $p=0.0002$ and $p=0.0002$ at 2, 24 and 48h respectively; **Fig. 1C**). Before plantar incision, baseline thermal withdrawal thresholds were not different between both genotypes (**Fig. 1D**). Following plantar incision, WT animals progressively exhibited significant thermal hyperalgesia from 24h to 48h post-

incision characterized by a significant decrease of thermal withdrawal thresholds compared to baseline (p=0.0003, p=0.007 at 24 and 48h respectively; **Fig. 1D**). TrkAC animals also developed significant thermal hyperalgesia from 24h to 48h post-incision similarly to WT (p=0.025, p=0.042 at 24 and 48h respectively; **Fig. 1D**).

Finally, we assessed referred mechanical allodynia using abdominal von Frey test following intraperitoneal administration of cyclophosphamide (CYP) or saline in WT and TrkAC mice (**Fig. 1E**). Before CYP injection, 50% mechanical withdrawal thresholds (*i.e.,* baseline) were not different between all groups and genotypes (WT and TrkAC). Saline administration did not significantly change mechanical thresholds in WT and TrkAC mice (**Fig. 1E**). However, following CYP administration, WT animals exhibited severe mechanical allodynia from 4h to 48h post-CYP which was characterized by a significant decrease of 50% mechanical threshold compared to WT saline group (p=0.029, p=0.002, p=0.037 at 4, 24 and 48h respectively; **Fig. 1E**). TrkAC mice treated with CYP also developed significant referred allodynia from 4h to 48h compared to WT saline treated mice, but to a smaller extent than WT CYP, since 50% mechanical threshold of TrkAC CYP mice was significantly different from WT CYP mice 4h and 24h following CYP administration (p=0.04, p=0.003 at 4 and 24h respectively; **Fig. 1E**).

To verify the development of cystitis, we evaluated bladder histology and cystometry parameters in WT and TrkAC mice following cystitis (see supplementary results). Overall, we did not observe any obvious anatomical difference of the bladder between WT and TrkAC saline treated mice (**supplementary Fig. 1A**). However, the bladder wall appeared thickened in WT CYP treated mice compared to WT saline group and was associated with partial loss of the urothelium (**supplementary Fig. 1A**). TrkAC CYP mice presented moderate mucosal ulceration, and mild to moderate oedema and haemorrhage compared to WT CYP group but were still significantly damaged compared to TrkAC and WT saline groups (**supplementary Fig. 1A**). We did not observed significant differences in the

alterations of the cystometry parameters induced by CYP administration between TrkAC and WT mice (**supplementary Fig. 1B, C&D and supplementary results for details**). Finally, since we observed this decrease of referred mechanical allodynia in TrkAC mice following cystitis, we assessed more directly mechanical visceral response to colonic distension in naive WT and TrkAC mice. TrkAC mice exhibited a significant decrease in visceromotor response to colonic distension at the highest volumes (*i.e.,* 80 and 100µl) compared to WT mice (p=0.021, p=0.015 at 80 and 100 µl, respectively; **supplementary Fig. 2A**).

Similar development of inflammation in WT and TrkAC mice following plantar incision or cystitis

As NGF is released following an injury and participates to inflammation through TrkA activation, we assessed paw thickness, bladder weight ratio and IL-6 paw skin and bladder contents following plantar incision and cystitis, respectively. The thickness of the ipsilateral hindpaw, assessed with a vernier caliper, significantly increased compared to the contralateral paw in WT and TrkAC mice in a similar manner 2h and 48h following plantar incision (p≤0.0001 for each time point and each group; **Fig. 2A**). For the cystitis model, the bladder weight/total weight ratio was similar between WT and TrkAC at 4h and 48h following saline administration (**Fig. 2B**). CYP injection significantly increased bladder weight in both WT and TrkAC, in a similar manner, at 4h (p=0.0005) and 4h and 48h (p≤0.0001 and p=0.02), respectively, compared to their respective control groups (**Fig. 2B**).

The increase of IL-6 content in the hindpaw skin and its kinetic were similar between both WT and TrkAC mice with a significant increase compared to the contralateral side from 2h to 48h after plantar incision where IL-6 content was still significantly increased compared to the contralateral paw in both genotypes (p≤0.0001

for both genotypes at 6h; p=0.049 and p=0.016 for WT ipsi and TrkAC ipsi at 48h, respectively; **Fig. 2C**). We also observed a similar increase of IL-6 bladder content 4h following CYP injection in WT and TrkAC groups compared to their control groups (p=0.024 and p=0.0008, respectively), which reached basal levels 48h after CYP injection (**Fig. 2D**).

We also assessed CGRP bladder innervation since it has been shown that CGRP staining in the bladder is increased following CYP treatment [15,49] and we previously demonstrated a decrease of free nerve endings in the skin of TrkAC mice. As expected, CGRP staining was significantly increased in the detrusor as well as the urothelium of WT CYP group compared to WT saline group (lower and upper left panel, respectively, **Fig. 2E & inset**). However, TrkAC saline mice already presented a significant decrease of CGRP staining especially in the urothelium, suggesting loss of fine peripheral peptidergic innervation (upper right panel, **Fig. 2E & inset**). Intriguingly, TrkAC CYP treated mice exhibited a further significant decrease of CGRP staining compared to WT saline group even in the detrusor (lower right panel, **Fig. 2E & inset**). Quantification of the percentage of CGRP staining confirmed a significant decrease of CGRP in TrkAC saline and CYP mice compared to WT saline mice (p=0.039 and p=0.008, respectively, **Fig. 2E, histogram**). CYP administration significantly increased CGRP staining only in WT but not TrkAC mice (p=0.041, **Fig. 2E, histogram**). To extend the decrease of fine peripheral innervation along the gastrointestinal tract, we also investigated CGRP staining in the colon. We observed a reduction of CGRP staining in the colon of naive TrkAC mice compared to WT mice (**supplementary Fig. 2B**), such as observed in the bladder of TrkAC and WT saline groups. By contrast, we did not observe any changes in CGRP and IB4 positive fibres staining in the dorsal horn of the spinal cord (**supplementary Fig. 3A**). Taken together, these results suggest that TrkAC mice

exhibit a specific decrease of mostly peptidergic free nerve endings compared to WT animals in visceral tissues as we previously described in the thick and thin glabrous skin.

Capsaicin-induced nocifensive behaviour and Ca^{2+} imaging response of DRG cells is similar between WT and TrkAC mice

Since a deficit in fine pepdidergic fibers which largely expressed the prototypic heat sensing receptor TRPV1 was observed in TrkAC mice, we assessed nocifensive behavioural responses (*i.e.,* licking, biting, lifting, and flinching of the left hindpaw) following intraplantar capsaicin administration (**Fig. 3A**). WT and TrkAC mice spent similar time in nocifensive behaviours (55.7 ± 5.5s and 59.8 ± 6s, respectively, p=0.621). We also measured the $[Ca^{2+}]_i$ on cultured DRG neurons in response to capsaicin. Interestingly, we observed a decrease of the number of capsaicin-responsive cells in TrkAC mice compared to WT mice (51% *vs* 33%, Chi2 square value p ≤0.0001, **Fig. 3B**). However, the peak intensity of the first calcium response following capsaicin was similar between WT and TrkAC DRG neurons while desensitization and probably tachyphylaxis phenomena following subsequent capsaicin applications seems significantly precocious in TrkAC mice compared to WT mice, at least following the second and third capsaicin applications (p ≤0.0001 and p=0.017, respectively, **Fig. 3C&D**).

Quantitative PCR of NGF/TrkA signalling pathways in DRGs following plantar incision or CYP administration in WT and TrkAC mice

Since NGF effect on genes expression in the DRG cell bodies is due to the trafficking of the NGF/TrkA complex from the periphery toward the DRG, we first assessed TrkA trafficking along the sciatic nerve 48h after plantar incision. The accumulation of TrkA receptors on the distal part of the ligature of the nerve 48h after plantar incision was

similar between WT and TrkAC, suggesting normal trafficking of NGF/TrkA complex along the sciatic nerve in TrkAC mice (**supplementary Fig. 3B**).

Forty eight hours following plantar incision, we observed a significant increase of Akt, Mapk14 (*i.e.* p38 MAPK) and Jun mRNA levels in the ipsilateral lumbar DRGs of WT mice compared to the contralateral side ($p \leq 0.0001$, **Table 3**). By contrast, this increase of Akt, Mapk14 and Jun mRNAs levels was absent in the ipsilateral DRGs of TrkAC mice and their expression levels were similar to those observed on the contralateral side as well as the contralateral DRGs of WT mice (**Table 3**). The expression levels of the others pathways investigated (Erk1, Erk2, Pkc, Pkmzeta and Pka) were not different between the ipsilateral and contralateral DRGs in WT and TrkAC mice as well as between both genotypes (**Table 3**). Finally, we observed no significant difference of Asic3 mRNA expression in the contralateral DRGs of TrkAC mice compared to the contralateral DRGs of WT mice, indicating similar expression of Asic3 at basal level between TrkAC and WT mice. However, a significant decrease of Asic3 mRNA expression in ipsilateral DRGs of WT mice compared to the contralateral side 48h post incision ($p=0.011$) was observed. In addition, we found a significant decrease of Asic3 mRNA level in the ipsilateral DRGs of TrkAC mice compared to the contralateral side and also to the contralateral DRGs of WT mice ($p=0.034$ and $p=0.0002$, respectively, **Table 3**).

By contrast to the plantar incision model, we did not observe any significant changes of Akt, Mapk14 (*i.e.* p38 MAPK),Jun, and Asic3 mRNA expression in the lumbar DRGs of WT CYP animals compared to WT control 48h following CYP administration (**Table 3**). The results were similar for the TrkAC mice with no significant increase in TrkAC CYP mice compared to TrkAC saline mice (**Table 3**).

Expression of phospho-AKT and phospho-P38 MAPK in the ipsilateral and contralateral lumbar DRGs of WT and TrkAC mice following paw incision

Our q-PCR data showed a significant increase of the levels of the transcripts especially encoding Akt and p38 MAPK, only in ipsilateral DRGs of WT mice following plantar incision. We therefore analysed by Western blotting, the expression of the activated form (*i.e.,* phosphorylated) of at least, AKT and P38 MAPK proteins in the contralateral and ipsilateral DRGs of WT and TrkAC mice 48h following plantar incision (**Fig. 4A,B,C&D**). The expression of p-AKT/total AKT in the DRGs was unchanged between both sides in WT and TrkAC groups and between genotypes (**Fig. 4A&B**). However, the expression of p-P38/totalP38 in the DRGs was significantly increased in the ipsilateral DRGs of WT mice compared to the contralateral side and TrkAC ipsilateral side ($p=0.004$ and $p=0.001$, respectively). This increase of P38 MAPK was not observed in the TrkAC mice such as found at the transcript level ($p=0.815$, **Fig. 4C&D**).

ASIC3, TrkA, CGRP expression in ipsilateral DRGs of WT and TrkAC mice following paw incision or cystitis

Since increase expression of ASIC3 has been observed following plantar incision in rat [10], NGF is a regulator of Asic3 gene expression through TrkA/JNK/p38 MAPK pathways [29] and, ASIC3 may participate to mechanotransduction phenomenon [27,38], we assessed the expression of ASIC3, TrkA and CGRP in ipsilateral L4-L5-L6 DRGs neurons 48h following plantar incision (**Fig. 5A,B&C**). The representative photomicrographs showed, from left to right, ASIC3, TrkA, CGRP and merge staining in ipsilateral DRGs of WT (upper panel) and TrkAC (lower panel) 48h following plantar incision (**Fig. 5A**). Arrows on the pictures indicate DRG neurons expressing both ASIC3, TrkA and CGRP which was decreased in TrkAC mice compared to WT. The percentage of TrkA and CGRP positive neurons was similar between WT and TrkAC mice following

plantar incision (29.8 ± 1.9% and 32.2 ± 3.2 % in WT *vs* 32.7 ± 3.1% and 26.7 ± 1% in TrkAC, respectively, **Fig. 5B**). However, the number of ASIC3 positive neurons was significantly decreased in TrkAC animals compared to WT following plantar incision (68 ± 4.5% *vs* 79.9 ± 5.1%, respectively, p=0.03 **Fig. 5B**). Importantly, this decrease of ASIC3 was found in CGRP (WT: 25.9 ± 4% *vs* TrkAC: 17.1 ± 1.7%, p=0.041) and TrkA/CGRP (WT: 21.1 ± 2.2% *vs* TrkAC: 14.6 ± 1.7%, p=0.028) positive neurons, respectively (**Fig. 5C**).

Since increase expression of ASIC3 has been observed following plantar incision, we also assessed its expression along with CGRP and TrkA in L6 DRG neurons 48h following saline or CYP. Representative photomicrographs showed an increase of the number of CGRP positive DRGs neurons specifically innervating the bladder only in WT CYP mice (**Fig. 6A**). Importantly, ASIC3/CGRP and ASIC3/TrkA/CGRP bladder co-expressing neurons were only increased in WT CYP mice but not in TrkAC CYP mice (**Fig. 6A**).

The average percentage of fluorogold positive neurons specifically innervating the bladder in L6 DRG was around 34% of the total number of DRG neurons which is like what has been reported previously [49,50]. This percentage was similar between WT and TrkAC mice (34 ± 2% and 35 ± 1%) and stayed unchanged following CYP administration, as expected (32.7 ± 2% and 32 ± 1.6% for WT CYP and TrkAC CYP, respectively). Among fluorogold positive neurons (*i.e.,* bladder innervating neurons) a vast majority, around 85%, expressed ASIC3 channels (**Fig. 6B**), which is similar to what has been observed previously [19]. This global expression of ASIC3 was the same between WT and TrkAC mice injected with saline and unchanged following CYP administration. Also in fluorogold positive neurons, around 40% of bladder neurons expressed TrkA **(Fig. 6B**). This expression of TrkA was similar between WT and TrkAC saline mice and stayed unchanged following CYP or saline administration. The percentage of bladder neurons

expressing CGRP was not different between WT and TrkA saline control groups (**Fig. 6B**). However, we observed a significant increase of the number of CGRP positive bladder neurons in WT CYP mice compared to WT saline group (50.5 ± 3% *vs* 40.5 ± 2.1%, respectively, p=0.037, **Fig. 6B**). We did not find such an increase in the TrkAC CYP group compared to TrkAC saline group (40.8 ± 6.5% *vs* 42.1 ± 6%, respectively, p=0.877, **Fig. 6B**).

We also observed a significant increase of ASIC3/CGRP positive bladder neurons in WT CYP group compared to WT saline group (41.9 ± 3% *vs* 28.7 ± 1.2%, respectively, p=0.015, **Fig. 6C**). There was no increase of this subtype of neurons in the TrkAC CYP group compared to TrkAC saline group (32.4 ± 4.2% *vs* 32 ± 2.1%, respectively, **Fig. 6C**) which is also not different from WT saline group. The number of TrkA/CGRP double positive bladder neurons was similar between WT and TrkAC saline mice and was not modified following CYP administration (**Fig. 6C**). However, we found a significant increase of the number of ASIC3/TrkA/CGRP triple positive bladder neurons in the WT CYP group compared to WT saline group (30.4 ± 6% *vs* 22.6 ± 2.8%, respectively, p=0.031, **Fig. 6C**). We did not observe such increase of this type of neurons in the TrkAC CYP group compared to TrkAC saline group (21.3 ± 2.1% *vs* 22.7 ± 1.9%, respectively, **Fig. 6C**), which is also not different from WT saline group.

Discussion

Here, we have confirmed and extended the specific lack of mechanical allodynia development in TrkAC mice following somatic and, to a lesser extent, visceral injuries. Thermal hyperalgesia development was unaffected, and despite a deficit of mostly peptidergic fibers innervation in somatic and visceral tissues, TrkAC and WT mice exhibited similar pain behaviours and calcium imaging response of DRG neurons following capsaicin. This specific loss of mechanical allodynia development in TrkAC mice was not associated with changes in different inflammatory parameters and NGF/TrkA trafficking. However, alterations in the expression/function of mainly two TrkA specific intracellular pathways (p38 MAPK and c-Jun) in the DRGs of TrkAC mice following plantar incision were observed, which ultimately lead to a reduction of, at least, ASIC3 channel expression in TrkA peptidergic neurons. Taken together, these results suggest that these two specific TrkA intracellular pathways, especially p38 MAPK, are probably very important for the development of mechanical allodynia at least following somatic injury and that ASIC3 might be a crucial player in both somatic and visceral pain conditions mediated by NGF/TrkA.

TrkAC mice present a specific and profound deficit in mechanical allodynia development after systemic NGF injection and plantar incision. Following cystitis, TrkAC mice exhibited a slight but significant reduction of referred mechanical hypersensitivity compared to WT mice. By contrast, cystometry parameters were similarly decreased in both genotypes following CYP administration as described previously in WT mice [45,46,52]. Moreover, colonic mechanical sensitivity assessed by colorectal distension was impaired in TrkAC mice compared to WT mice. Alterations in the development of peripheral inflammation cannot explain the mechanical allodynia deficit in TrkAC mice since a similar increase of different inflammatory parameters

following somatic or visceral injuries was observed between TrkAC and WT mice as described previously [1,8,17,43]. However, a decrease in the density of CGRP-positive fibres in the bladder and the colon of TrkAC mice, as well as an absence of an increase of CGRP bladder staining following CYP in TrkAC mice compared to WT was observed, suggesting a specific reduction in peripheral, mostly peptidergic, innervation in visceral tissues similar to what we have previously described in the skin [16]. Thus, TrkAC mice present specific developmental target innervation defects of mostly peptidergic terminal branches in both somatic and visceral tissues, well known to be highly dependent on NGF [9,25,34]. Therefore, an obvious explanation for the specific loss of mechanical allodynia in TrkAC mice could be this peripheral innervation defect. However, these peptidergic fibres, expressing mainly TRPV1, are dispensable for mechanically-evoked behaviours, but are essential for behaviours evoked by noxious heat [6]. Indeed, NGF-induced heat hyperalgesia is absent in TRPV1 knock-out mice or after TRPV1 blockade [5]. Nonetheless, thermal hyperalgesia was totally preserved in TrkAC mice at baseline and following systemic NGF administration or plantar incision. TrkAC mice could rather display a functional deficit of TRPV1. However, basal TRPV1 expression in lumbar DRG is unaltered in TrkAC mice [16], and they exhibit similar nocifensive behavioural responses following capsaicin and calcium imaging DRGs neuronal response after the first capsaicin application compared to WT mice. Finally, despite significant reduction in the density of epidermal neuritis including peptidergic fibres, mice lacking $p75^{NTR}$, the pan receptor of neurotrophins, still developed mechanical and thermal hyperalgesia after systemic NGF delivery while they exhibited a decrease in basal mechanical and thermal thresholds [2,3]. By contrast, TrkAC mice did not display any changes in basal mechanical and thermal thresholds despite reduction in the density of epidermal and visceral innervation but

only a specific loss of mechanical allodynia development following somatic and, to a lesser extent, visceral injuries. We have also previously shown that the expression of some subtypes of important peripheral mechanosensory fibres (TrkB and early Ret positive fibres) were unaffected in TrkAC mice. Therefore, this marked decrease in peripheral innervation cannot explain by its own the lack of mechanical allodynia development in TrkAC mice, especially following somatic injury.

Thus, another possibility is that the remaining primary afferents fibres, important in the development of mechanical allodynia, present a specific functional silencing due to the absence of TrkA specific pathways. By contrast, an increase activation of TrkC specific pathways and/or TrkA and TrkC intracellular signalling pathways largely overlap, to mediate thermal hyperalgesia. Alternatively, it has been shown that acute noxious heat sensing in mice depends on a triad of transient receptor potential ion channels (TRPM3, TRPV1 and TRPA1), which are not expressed solely in TrkA positive neurons [47,48]. Consequently, we assessed the mRNA expression of several common and specific TrkA/TrkC intracellular transduction pathways in the DRGs after plantar incision or CYP in WT and TrkAC mice. The basal mRNA expression of all the pathways investigated were similar between both genotypes, suggesting that the expression of TrkAC did not modified significantly the overall NGF/TrkA signalling of DRG cells in basal conditions. However, following plantar incision, there was a marked decrease of the up-regulation of Akt, p38 MAPK and c-Jun mRNA expression in the ipsilateral DRGs of TrkAC mice compared to WT. At the protein level, we also demonstrated an absence of increased phosphorylation of p38 MAPK in TrkAC mice compared to WT. Interestingly, the mRNA expression of the same pathways was not modified following CYP in WT mice as well as TrkAC mice, suggesting that these pathways are mainly involved in the development of somatic mechanical allodynia.

These changes of some pathways, such as p38 MAPK, between WT and TrkAC mice may be due to few proteins, which bind differentially to the intracellular domains of TrkA and TrkC receptors [20,35,36], leading to the modulation of distinct downstream pathways. Alternatively, structural differences between TrkA and TrkAC receptors could lead to different activation levels of downstream effectors [31]. Some of these pathways (*i.e*, PI3K, p38 MAPK) have been already involved in the development of NGF induced hyperalgesia but typically following intraplantar administration of the specific inhibitors of these pathways and tested either on thermal or mechanical hyperalgesia [56]. Thus, changes of a set of intracellular pathways including p38 MAPK and probably c-Jun could be specifically involved in NGF-induced mechanical allodynia. Overall, changes of intracellular pathways and probably, genes expression in the DRG, seem essential for the development of mechanical allodynia induced by NGF while thermal hyperalgesia could be mainly due to peripheral sensitization of heat transducers in primary afferent terminals.

The expression/function of the mechanostransducer(s) involved in the development of mechanical allodynia at the periphery is largely dependent on NGF, and several candidates have been proposed [13]. ASIC3, a proton gated channel, seems to be an important contributor of the nociceptor mechanosensory function and, importantly, its expression is regulated by NGF and particularly TrkA transduction pathways [30]. Interestingly, we found a decrease in the up-regulation of ASIC3 protein expression in TrkA-positive DRGs neurons in TrkAC mice following both somatic and visceral injuries. At the mRNA level, we observed a decrease of Asic3 expression in the ipsilateral DRG of WT mice only following paw incision, which could indicate increased translation. A further decrease of Asic3 mRNA in the ipsilateral DRG of TrkAC mice was also found. Despite an increase translation of Asic3 in TrkAC mice

such as in WT, the level of Asic3 mRNA in the ipsilateral DRG could be too low to observe a significant increase of ASIC3 protein expression. This decrease of ASIC3 expression could partially explain the lack of mechanical allodynia development in TrkAC mice, but we cannot exclude the involvement of others mechanotransducers. Nonetheless, ASIC3 has been already involved in mechanical hypersensitivity in several types of somatic pain models [11,12,42,51], and recently, Zhou *et al.* [55] demonstrated that NGF-induced hyperalgesia following repeated dural infusions of an inflammatory soup, seems dependent on ASIC3 expression in the trigeminal nucleus caudalis. Several studies also support an important contribution of ASIC3 in visceromechanosensitivity but also TRPV1, contrasting to somatic mechanosensitivity [19, 20, 38]. This differential contribution of TRPV1 between visceral and somatic mechanosensitivities could explain the partial decrease of referred mechanical allodynia in TrkAC mice following CYP. Finally, Mamet *et al.,* demonstrated that ASIC3 overexpression by NGF was dependent on the cooperation of JNK (c-Jun)/p38 MAPK pathways [30]. Strikingly, we observed a decreased expression of these two specific pathways in the DRGs of TrkAC mice associated with a decrease of ASIC3 expression, which could finally lead to mechanical allodynia deficit in chronic pain states especially following somatic injuries. Mechanotransduction is a complex phenomenon especially in mechanical allodynia. Consequently, others contributors of the nociceptor mechanosensory function could be also at play.

Thus, we have demonstrated a specific deficit of mechanical allodynia development in TrkAC mice following somatic and to a lesser extent, visceral injuries. This deficit does not seem to be due to the peripheral innervation defects in the skin and visceral tissues of TrkAC mice but rather an alteration of TrkA specific transduction pathways. Changes in the expression of different transduction pathways, especially

p38 MAPK, were observed, which could ultimately lead to a specific deficit of mechanical allodynia development through a decrease of, at least, ASIC3 expression, especially after somatic injury. Further studies are needed to better clarify this differential role of TrkA specific transduction pathways in mechanical allodynia and thermal hyperalgesia, where the TrkAC mice could be a very valuable tool.

Acknowledgements

This work was supported by Inserm, Conseil Régional Auvergne-Rhône-Alpes (project Ressourcement S3, Arth-Innov) and Feder as well as the French government IDEX-ISITE initiative 16-IDEX-0001 (CAP 20-25).

.

Declaration of Interests

All authors have read and agreed to the contents of the manuscript and have no competing financial interests.

Figures legends

Figure 1: **Specific lack of mechanical allodynia in TrkAC mice especially following somatic injuries**

Effect of systemic injection of NGF (1 mg/kg, s.c. at 0.1mL/10g) in WT and TrkAC mice on mechanical allodynia (**A**) and thermal hyperalgesia (**C**) using von Frey test (up and down method) and thermal plantar test, respectively. Mechanical allodynia and thermal hyperalgesia were assessed before, 4h, 6h and 24h and before, 1h, 6h and 24h, respectively, following systemic NGF injection. Effect of plantar incision in WT and TrkAC mice on mechanical allodynia (**B**) and thermal hyperalgesia (**D**) using von Frey test (up and down method) and thermal plantar test, respectively. Pain behaviours were assessed before, 2h, 24h and 48h after plantar incision of the left hind paw. (**E**) Effect of cyclophosphamide induced-cystitis on referred mechanical allodynia in WT and TrkAC mice. Referred mechanical allodynia was assessed by the application of von Frey hairs on the abdomen using the up and down method before, 4h, 24h and 48h after a single intraperitoneal injection of cyclophosphamide (CYP: 150 mg/kg) or saline in WT and TrkAC female mice. n=13-15 animals per group and conditions (*i.e.,* paw incision or CYP administration) and n=8 per group for systemic NGF model; A, B, C, D and E. Two-way repeated measures ANOVA followed by a Tukey post hoc test. A, B, C, D * $p \leq 0.05$, ** $p \leq 0.01$, *** $p \leq 0.001$ compared to the baseline values of WT or TrkAC groups, ° $p \leq 0.05$, °° $p \leq 0.01$, °°° $p \leq 0.001$ compared to WT group. E * $p \leq 0.05$, ** $p \leq 0.01$, compared to WT saline group, $^{\#}$ $p \leq 0.05$ compared to WT CYP group.

Figure 2: **No difference in inflammatory reaction following injuries between TrkAC and WT mice despite peripheral deficit of CGRP innervation in TrkAC mice** (**A**) Assessment of the ipsilateral (left) and contralateral (right) hind paws thickness 2h and 48h following plantar incision in WT and TrkAC mice using a Vernier calliper. (**B**) Temporal expression profile of interleukin 6 (IL-6) in skin of the ipsilateral (left) and contralateral (right) hind paws 2h and 48h after plantar incision in WT and TrkAC mice. (**C**) Assessment of the bladder/total mice weight ratio 4h and 48h following injection of saline or CYP (150 mg/kg, i.p.) in WT and TrkAC female mice. (**D**) Temporal expression profile of interleukin 6 (IL-6) in the bladder 4h and 48h following injection of vehicle or CYP in WT and TrkAC mice. Results are shown as the average of IL-6 content pg per milligram of total tissue protein. n=5 per group and conditions (*i.e.,* paw incision or CYP administration) and time point. Two-way ANOVA followed by a Tukey post hoc test. * $p \leq 0.05$, *** $p \leq 0.001$ compared to the contralateral side and to WT animals. (**E**) Left panel: Representative photomicrographs of CGRP bladder wall staining in female WT and TrkAC mice 48h after injection of saline or CYP (150 mg/kg, i.p.). Inset. High power image of CGRP staining of the bladder wall. Harrowhead showing a decrease of CGRP staining in the bladder wall. Right panel: Histogram of the percentage of CGRP staining on the total bladder surface in WT and TrkAC female mice 48h after injection of vehicle or CYP (n=4-5 in each group). One-way ANOVA followed by a Tukey post hoc test. °$p \leq 0.05$ compared to the WT vehicle group. * $p \leq 0.05$, ** $p \leq 0.01$ compared to the WT saline and CYP groups.

Figure 3: **No changes in behavioural and Ca^{2+} imaging responses of DRG neurons following TRPV1 activation**

Effect of intraplantar capsaicin injection (1.5µg/20µL/mice) in WT and TrkAC mice (**A**). Time spent (s) in spontaneous nocifensive behaviours (*i.e.* licking, biting, lifting, and flinching) of the injected paw was assessed for 5 minutes following capsaicin injection. Student *t* test between WT and TrkAC groups (n=6-7 per group). (**B**) Percentage of DRG cells responsive or not to capsaicin stimulation between WT and TrkAC mice following calcium imaging. (**C**) Ratio of calcium-dependent fluorescence, F340/380, as a function of time from primary culture DRGs cells following pulses of capsaicin (100 nM, applied as shown at top) for 15s with a 4min interval between each stimulation. At the end of the experiment all excitable cells were identified by the application of high-KCl Krebs-Ringer solution for 1min. (**D**) Histogram of peak intensity for each of the five capsaicin stimulations. For peak intensity calculation, the ratio value just prior to the start of the stimulus was subtracted from the maximum ratio value within the 80 seconds following capsaicin application. Only cells displaying an increase of at least 15% of their peak intensity in response to KCl were included for analysis (n=257 cells for WT and n=377 cells for TrkAC). Two-way ANOVA followed by a Sidak's multiple comparison post hoc test. * $p \leq 0.05$, *** $p \leq 0.001$ compared to WT.

Figure 4: **Lack of increase of p-P38MAPK expression in the ipsilateral DRG of TrkAC mice following plantar incision**

Expression of phospho Ser473-AKT, total AKT, phospho Thr180/Tyr182-P38 MAPK, total P38 MAPK proteins in ipsilateral and contralateral lumbar DRGs of WT and TrkAC mice 48h following plantar incision. Representative Western blot (**A&C**) and quantification histograms of phospho-AKT and total AKT (**B**) and phospho-P38 and

total P38 (**D**) of WT and TrkAC mice following plantar incision. All phospho bands of p-AKT and p-P38 were normalized relative to total AKT or P38 proteins, respectively, and expressed as a ratio. n=10 for each group. One-way ANOVA followed by a Tukey post hoc test. ** $p \leq 0.01$ compared to contralateral WT group, °° $p \leq 0.01$ compared to TrkAC mice.

Figure 5: **Decrease of ASIC3/TrkA/CGRP positive DRG neurons in TrkAC mice following plantar incision**

Analysis of ASIC3, TrkA and CGRP expression in sensory neurons of the L4-L5-L6 ipsilateral DRG 48h following plantar incision in WT and TrkAC mice. (**A**) From left to right, representative photomicrographs of ASIC3 (green), TrkA (red) and CGRP (grey) positive neurons in L4-L5-L6 DRGs of WT (upper panel) and TrkAC (lower panel) mice. Merge images (extreme right) show ASIC3-positive neurons expressing TrkA and CGRP (arrowhead; scale bar, 100µm). (**B**) Percentage of ASIC3, TrkA or CGRP positive neurons / number of total lumbar DRG neurons in WT and TrkAC mice. (**C**) Percentage of double or triple labelled lumbar DRG neurons / number of total lumbar DRG neurons in WT and TrkAC mice. 4-6 sections for each animal, n=5 per group (*i.e.,* ipsilateral and contralateral WT and TrkAC). Non parametric Mann-Whitney test. * $p \leq 0.05$ compared to WT animals.

Figure 6: **Lack of increase of ASIC3/TrkA/CGRP positive DRG neurons specifically innervating the bladder in TrkAC mice following cystitis**

Analysis of ASIC3, CGRP and TrkA expression in sensory neurons of the L6 DRG innervating the bladder 48h following saline or CYP injection in WT and TrkAC mice.

(**A**) From left to right, representative photomicrographs of fluorogold-positive neurons retrogradely labelled from the bladder wall (blue), ASIC3 (green), CGRP (grey) and TrkA (red) positive neurons in L6 DRG, from top to bottom, of WT vehicle, TrkAC vehicle, WT CYP and TrkAC CYP mice. Merge image (right) shows ASIC3-positive neurons expressing or not expressing TrkA and CGRP. (**B**) Percentage of fluorogold positive neurons expressing ASIC3, TrkA and CGRP in WT and TrkAC mice 48h following saline or CYP. (**C**) Percentage of double or triple labelled fluorogold positive neurons of L6 DRG in WT and TrkAC mice. Results are expressed as a percentage of fluorogold positive neurons. 4-6 sections for each animal, n=5 per group (*i.e.,* WT saline, TrkAC saline, WT CYP and TrkAC CYP). Non parametric Mann-Whitney test. * $p \leq 0.05$ compared to WT saline treated animals.

Table 1: List of primer sequences used for the q-PCR experiments.

Table 2: List of primary and secondary antibodies, dilutions and manufacturers used for the immunohistochemistry experiments.

Table 3: Gene expression profiling of TrkA, TrkC transduction pathways in the lumbar L4-L5-L6 DRGs of WT and TrkAC animals 48h following plantar incision or lumbar L6-S1 DRGs of WT and TrkAC animals 48h following saline or CYP injection. Relative quantity of the transcripts (mean +/-SEM) expressed in the ipsilateral and contralateral lumbar DRGs between WT and TrkAC mice assessed by q-PCR following incision (first part of the table “incision”). * $p \leq 0.05$ from the RQ of the contralateral WT DRG; ° $p \leq 0.05$ from the RQ of the contralateral TrkAC DRG. n=3-5 per group for the paw incision model. Non parametric Mann-Whitney test. Relative quantity of the transcripts (mean

+/- SEM) expressed in the lumbar DRGs between WT saline or WT CYP and TrkAC saline or TrkAC CYP mice assessed by q-PCR (second part of the table “cystitis”). * p ≤ 0.05 from the RQ of the contralateral WT DRG. n=4-6 per group for CYP model. Non parametric Mann-Whitney test.

Supplementary legends

Supplementary Figure 1: (**A**) Representative photomicrographs of Hematoxyline/Eosine bladder histology in female WT and TrkAC mice 48h after injection of saline or CYP (150 mg/kg, i.p.). (**B**) Representative typical recordings of several micturition cycle in anesthetised WT and TrkAC female mice 48 h after injection of saline or CYP. (**C**) Histograms of cystometry parameters analysis ((intercontraction interval (min), bladder capacity (µl), mean voiding volume (µl): from left to right)). (**D**) Maximum bladder pressure, contraction threshold, resting pressure, contraction amplitude in anesthetised female WT and TrkAC mice 48 h following injection of saline or CYP. n=5-6 for each group and genotype. One-way ANOVA followed by a Tukey post hoc test. * $p \leq 0.05$ compared to WT group.

Supplementary Figure 2: (**A**) Visceromotor response (VMR) to colorectal distension (CRD) in naïve WT and TrkAC mice (left panel, n=8 per genotype). Right panel: the area under the curve (AUC) was calculated between 20 µL and 100 µL for WT and TrkAC groups. (**B**) Representative photomicrographs of CGRP colon wall staining in naïve WT and TrkAC mice (n=4 for each genotype).

Supplementary Figure 3: (**A**) Representative photomicrographs of TrkA trafficking along the sciatic nerve in WT (left panel) and TrkAC (right panel) mice 48h following plantar incision. TrkA receptor is accumulated in a similar manner between WT and TrkAC at the distal side of the ligation 48h following plantar incision (scale bar, 100µm). n=2 for each genotype. (**B**) Representative photomicrographs of non peptidergic (IB4-positive, green) and peptidergic (CGRP-positive, red) positive fibres in the lumbar

spinal cord in naïve WT and TrkAC mice. Both types of fibres normally innervate adult spinal cord in TrkAC compared to WT mice (n=2 for each genotype; scale bar, 200μm).

References

[1] Banik RK, Subieta AR, Wu C, Brennan TJ. Increased nerve growth factor after rat plantar incision contributes to guarding behavior and heat hyperalgesia. Pain 2005;117:68–76.

[2] Bergmann I, Priestley J V., McMahon SB, Bröcker EB, Toyka K V., Koltzenburg M. Analysis of cutaneous sensory neurons in transgenic mice lacking the low affinity neurotrophin receptor p75. Eur J Neurosci 1997;9:18–28.

[3] Bergmann I, Reiter R, Toyka K V, Koltzenburg M. Nerve growth factor evokes hyperalgesia in mice lacking the low-affinity neurotrophin receptor p75. Neurosci Lett 1998;255:87–90.

[4] Brennan TJ, Vandermeulen EP, Gebhart GF. Characterization of a rat model of incisional pain. Pain 1996;64:493–501.

[5] Caterina MJ, Leffler A, Malmberg AB, Martin WJ, Trafton J, Petersen-Zeitz KR, Koltzenburg M, Basbaum AI, Julius D. Impaired nociception and pain sensation in mice lacking the capsaicin receptor. Science 2000;288:306–313.

[6] Cavanaugh DJ, Lee H, Lo L, Shields SD, Zylka MJ, Basbaum AI, Anderson DJ. Distinct subsets of unmyelinated primary sensory fibers mediate behavioral responses to noxious thermal and mechanical stimuli. Proc Natl Acad Sci U S A 2009;106:9075–80.

[7] Chaplan SR, Bach FW, Pogrel JW, Chung JM, Yaksh TL. Quantitative assessment of tactile allodynia in the rat paw. J Neurosci Methods 1994;53:55–63.

[8] Coelho A, Wolf-Johnston AS, Shinde S, Cruz CD, Cruz F, Avelino A, Birder LA. Urinary bladder inflammation induces changes in urothelial nerve growth factor and TRPV1 channels. Br J Pharmacol 2015;172:1691–1699.

[9] Denk F, Bennett DL, McMahon SB. Nerve Growth Factor and Pain Mechanisms. Annu Rev Neurosci 2017.

[10] Deval E, Noël J, Gasull X, Delaunay A, Alloui A, Friend V, Eschalier A, Lazdunski M, Lingueglia E. Acid-sensing ion channels in postoperative pain. J Neurosci Off J Soc Neurosci 2011;31:6059–6066.

[11] Deval E, Noel J, Gasull X, Delaunay A, Alloui A, Friend V, Eschalier A, Lazdunski M, Lingueglia E. Acid-Sensing Ion Channels in Postoperative Pain. J Neurosci 2011;31:6059–6066.

[12] Deval E, Noël J, Lay N, Alloui A, Diochot S, Friend V, Jodar M, Lazdunski M, Lingueglia E. ASIC3, a sensor of acidic and primary inflammatory pain. EMBO J 2008;27:3047–3055.

[13] Di Castro A, Drew LJ, Wood JN, Cesare P. Modulation of sensory neuron mechanotransduction by PKC- and nerve growth factor-dependent pathways. Proc Natl Acad Sci U S A 2006;103:4699–4704.

[14] Dixon WJ. Efficient Analysis of Experimental Observations. Annu Rev Pharmacol Toxicol 1980;20:441–462.

[15] Gonzalez EJ, Peterson A, Malley S, Daniel M, Lambert D, Kosofsky M, Vizzard MA. The effects of tempol on cyclophosphamide-induced oxidative stress in rat micturition reflexes. ScientificWorldJournal 2015;2015:545048.

[16] Gorokhova S, Gaillard S, Urien L, Malapert P, Legha W, Baronian G, Desvignes J-P, Alonso S, Moqrich A. Uncoupling of molecular maturation from peripheral target innervation in nociceptors expressing a chimeric TrkA/TrkC receptor. PLoS Genet 2014;10:e1004081.

[17] Guerios SD, Wang Z-Y, Bjorling DE. Nerve growth factor mediates peripheral mechanical hypersensitivity that accompanies experimental cystitis in mice. Neurosci Lett 2006;392:193–197.

[18] Hargreaves K, Dubner R, Brown F, Flores C, Joris J. A new and sensitive method for measuring thermal nociception in cutaneous hyperalgesia. Pain 1988;32:77–88.

[19] Hughes PA, Brierley SM, Young RL, Blackshaw LA. Localization and comparative analysis of acid-sensing ion channel (ASIC1, 2, and 3) mRNA expression in mouse colonic sensory neurons within thoracolumbar dorsal root ganglia. J Comp Neurol 2007;500:863–875.

[20] Kato H, Ohno K, Hashimoto K, Sato K. Synectin in the nervous system: expression pattern and potential as a binding partner of neurotrophin receptors. FEBS Lett 2004;572:123–128.

[21] Kays J, Zhang YH, Khorodova A, Strichartz G, Nicol GD. Peripheral Synthesis of an Atypical Protein Kinase C Mediates the Enhancement of Excitability and the Development of Mechanical Hyperalgesia Produced by Nerve Growth Factor. Neuroscience 2018;371:420–432.

[22] Kerr BJ, Souslova V, McMahon SB, Wood JN. A role for the TTX-resistant sodium channel Nav 1.8 in NGF-induced hyperalgesia, but not neuropathic pain. Neuroreport 2001;12:3077–80.

[23] Klesse LJ, Parada LF. Trks: signal transduction and intracellular pathways. Microsc Res Tech 1999;45:210–216.

[24] Lai HH, Shen B, Vijairania P, Zhang X, Vogt SK, Gereau RW. Anti-vascular endothelial growth factor treatment decreases bladder pain in cyclophosphamide cystitis: a Multidisciplinary Approach to the Study of Chronic Pelvic Pain (MAPP) Research Network animal model study. BJU Int 2017.

[25] Lewin GR, Lechner SG, Smith ESJ. Nerve growth factor and nociception: from experimental embryology to new analgesic therapy. Handb Exp Pharmacol 2014;220:251–82.

[26] Lewin GR, Ritter AM, Mendell LM. Nerve growth factor-induced hyperalgesia in the neonatal and adult rat. J Neurosci Off J Soc Neurosci 1993;13:2136–48.

[27] Lin S-H, Cheng Y-R, Banks RW, Min M-Y, Bewick GS, Chen C-C. Evidence for the involvement of ASIC3 in sensory mechanotransduction in proprioceptors. Nat Commun 2016;7:11460.

[28] Malik-Hall M, Dina OA, Levine JD. Primary afferent nociceptor mechanisms mediating NGF-induced mechanical hyperalgesia. Eur J Neurosci 2005;21:3387–94.

[29] Mamet J, Lazdunski M, Voilley N. How nerve growth factor drives physiological and inflammatory expressions of acid-sensing ion channel 3 in sensory neurons. J Biol Chem 2003;278:48907–13.

[30] Mamet J, Lazdunski M, Voilley N. How nerve growth factor drives physiological and inflammatory expressions of acid-sensing ion channel 3 in sensory neurons. J Biol Chem 2003;278:48907–48913.

[31] Markus A, Zhong J, Snider WD. Raf and akt mediate distinct aspects of sensory axon growth. Neuron 2002;35:65–76.

[32] Miller RE, Block JA, Malfait A-M. Nerve growth factor blockade for the management of osteoarthritis pain: what can we learn from clinical trials and preclinical models? Curr Opin Rheumatol 2017;29:110–118.

[33] Minden A, Lin A, McMahon M, Lange-Carter C, Dérijard B, Davis RJ, Johnson GL, Karin M. Differential activation of ERK and JNK mitogen-activated protein kinases by Raf-1 and MEKK. Science 1994;266:1719–1723.

[34] Mizumura K, Murase S. Role of Nerve Growth Factor in Pain. Handbook of experimental pharmacology.2015, Vol. 227. pp. 57–77.

[35] Mortimer D, Pujic Z, Vaughan T, Thompson AW, Feldner J, Vetter I, Goodhill GJ. Axon guidance by growth-rate modulation. Proc Natl Acad Sci U S A 2010;107:5202–5207.

[36] Nakamura T, Komiya M, Sone K, Hirose E, Gotoh N, Morii H, Ohta Y, Mori N. Grit, a GTPase-activating protein for the Rho family, regulates neurite extension through association with the TrkA receptor and N-Shc and CrkL/Crk adapter molecules. Mol Cell Biol 2002;22:8721–8734.

[37] O'Brien DE, Brenner DS, Gutmann DH, Gereau RW. Assessment of pain and itch behavior in a mouse model of neurofibromatosis type 1. J Pain Off J Am Pain Soc 2013;14:628–637.

[38] Page AJ, Brierley SM, Martin CM, Price MP, Symonds E, Butler R, Wemmie JA, Blackshaw LA. Different contributions of ASIC channels 1a, 2, and 3 in gastrointestinal mechanosensory function. Gut 2005;54:1408–1415.

[39] Patapoutian A, Reichardt LF. Trk receptors: mediators of neurotrophin action. Curr Opin Neurobiol 2001;11:272–280.

[40] Petty BG, Cornblath DR, Adornato BT, Chaudhry V, Flexner C, Wachsman M, Sinicropi D, Burton LE, Peroutka SJ. The effect of systemically administered recombinant human nerve growth factor in healthy human subjects. Ann Neurol 1994;36:244–246.

[41] Rice ASC, Cimino-Brown D, Eisenach JC, Kontinen VK, Lacroix-Fralish ML, Machin I, Mogil JS, Stöhr T. Animal models and the prediction of efficacy in clinical trials of analgesic drugs: a critical appraisal and call for uniform reporting standards. Pain 2008;139:243–247.

[42] Rudan I, Sidhu S, Papana A, Meng S-J, Xin-Wei Y, Wang W, Campbell-Page RM, Demaio AR, Nair H, Sridhar D, Theodoratou E, Dowman B, Adeloye D, Majeed A, Car J, Campbell H, Wang W, Chan KY, Global Health Epidemiology Reference Group (GHERG) GHERG. Prevalence of rheumatoid arthritis in low- and middle-income countries: A systematic review and analysis. J Glob Health 2015;5:010409.

[43] Sahbaie P, Shi X, Guo T-Z, Qiao Y, Yeomans DC, Kingery WS, Clark JD. Role of substance P signaling in enhanced nociceptive sensitization and local cytokine production after incision. Pain 2009;145:341–349.

[44] Sakurada T, Katsumata K, Tan-No K, Sakurada S, Kisara K. The capsaicin test in mice for evaluating tachykinin antagonists in the spinal cord. Neuropharmacology 1992;31:1279–1285.

[45] Silva RBM, Sperotto NDM, Andrade EL, Pereira TCB, Leite CE, de Souza AH, Bogo MR, Morrone FB, Gomez M V., Campos MM. Spinal blockage of P/Q- or N-type voltage-gated calcium channels modulates functional and symptomatic changes related to haemorrhagic cystitis in mice. Br J Pharmacol 2015;172:924–939.

[46] Studeny S, Cheppudira BP, Meyers S, Balestreire EM, Apodaca G, Birder LA, Braas KM, Waschek JA, May V, Vizzard MA. Urinary bladder function and somatic sensitivity in vasoactive intestinal polypeptide (VIP)-/- mice. J Mol Neurosci MN 2008;36:175–187.

[47] Usoskin D, Furlan A, Islam S, Abdo H, Lönnerberg P, Lou D, Hjerling-Leffler J, Haeggström J, Kharchenko O, Kharchenko P V, Linnarsson S, Ernfors P. Unbiased classification of sensory neuron types by large-scale single-cell RNA sequencing. Nat Neurosci 2015;18:145–53.

[48] Vandewauw I, De Clercq K, Mulier M, Held K, Pinto S, Van Ranst N, Segal A, Voet T, Vennekens R, Zimmermann K, Vriens J, Voets T. A TRP channel trio mediates acute noxious heat sensing. Nature 2018;555:662–666.

[49] Vizzard MA. Alterations in neuropeptide expression in lumbosacral bladder pathways following chronic cystitis. J Chem Neuroanat 2001;21:125–138.

[50] Vizzard MA, Erdman SL, de Groat WC. Increased expression of neuronal nitric oxide synthase (NOS) in visceral neurons after nerve injury. J Neurosci Off J Soc Neurosci 1995;15:4033–4045.

[51] Walder RY, Rasmussen LA, Rainier JD, Light AR, Wemmie JA, Sluka KA. ASIC1 and ASIC3 Play Different Roles in the Development of Hyperalgesia Following Inflammatory Muscle Injury. J Pain Off J Am Pain Soc 2010;11:210–218.

[52] Wang H-J, Lee W-C, Tyagi P, Huang C-C, Chuang Y-C. Effects of low energy shock wave therapy on inflammatory moleculars, bladder pain, and bladder function in a rat cystitis model. Neurourol Urodyn 2017;36:1440–1447.

[53] Xing J, Kornhauser JM, Xia Z, Thiele EA, Greenberg ME. Nerve growth factor activates extracellular signal-regulated kinase and p38 mitogen-activated protein kinase pathways to stimulate CREB serine 133 phosphorylation. Mol Cell Biol 1998;18:1946–1955.

[54] York RD, Molliver DC, Grewal SS, Stenberg PE, McCleskey EW, Stork PJ. Role of phosphoinositide 3-kinase and endocytosis in nerve growth factor-induced extracellular signal-regulated kinase activation via Ras and Rap1. Mol Cell Biol 2000;20:8069–8083.

[55] Zhou H, Wang X, Wang S, Liu C, Fu Q, Qin G, Zhou J, Chen L. Inhibition of Nerve Growth Factor Signaling Alleviates Repeated Dural Stimulation-induced Hyperalgesia in Rats. Neuroscience 2019;398:252–262.

[56] Zhuang Z-Y, Xu H, Clapham DE, Ji R-R. Phosphatidylinositol 3-Kinase Activates ERK in Primary Sensory Neurons and Mediates Inflammatory Heat Hyperalgesia through TRPV1 Sensitization. J Neurosci 2004;24:8300–8309.

[57] Zimmermann M. Ethical guidelines for investigations of experimental pain in conscious animals. Pain 1983;16:109–110.

Summary: Using TrkAC knock-in mice, we demonstrated a crucial role of c-Jun/p38MAPK/ASIC3 pathways specifically activated by NGF through TrkA for mechanical allodynia development

Figure 1

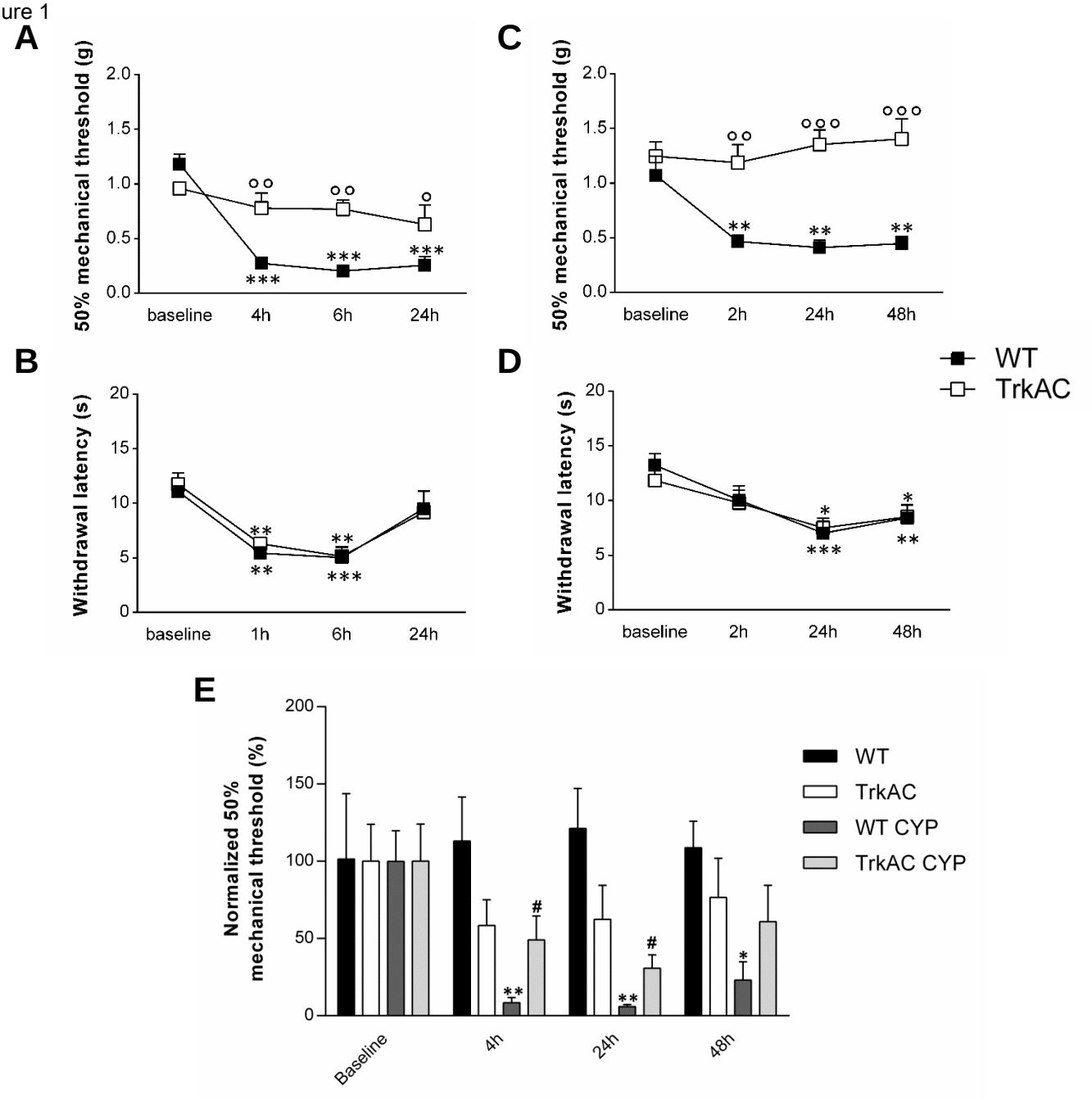

Figure 1

Figure 2

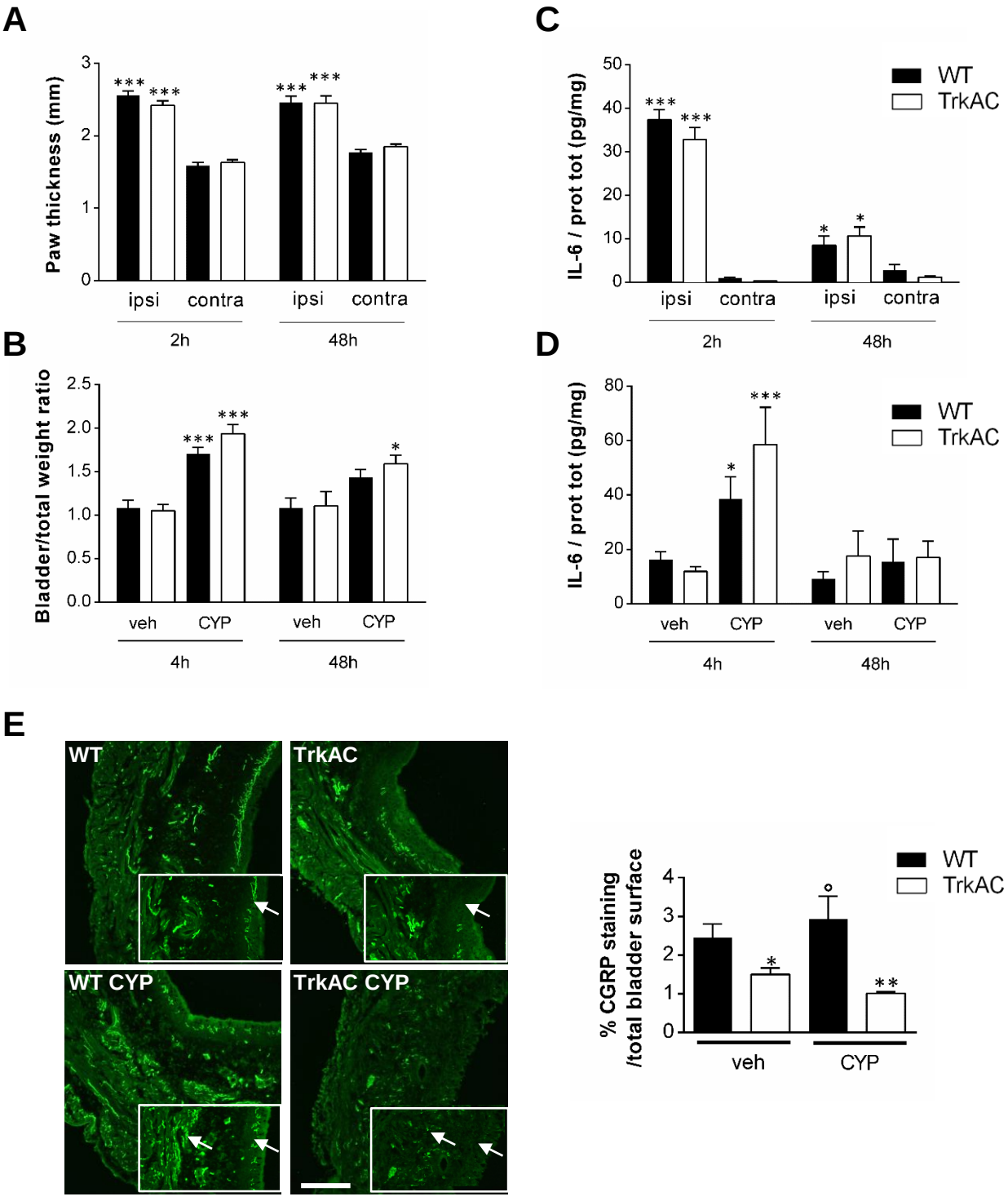

Figure 2

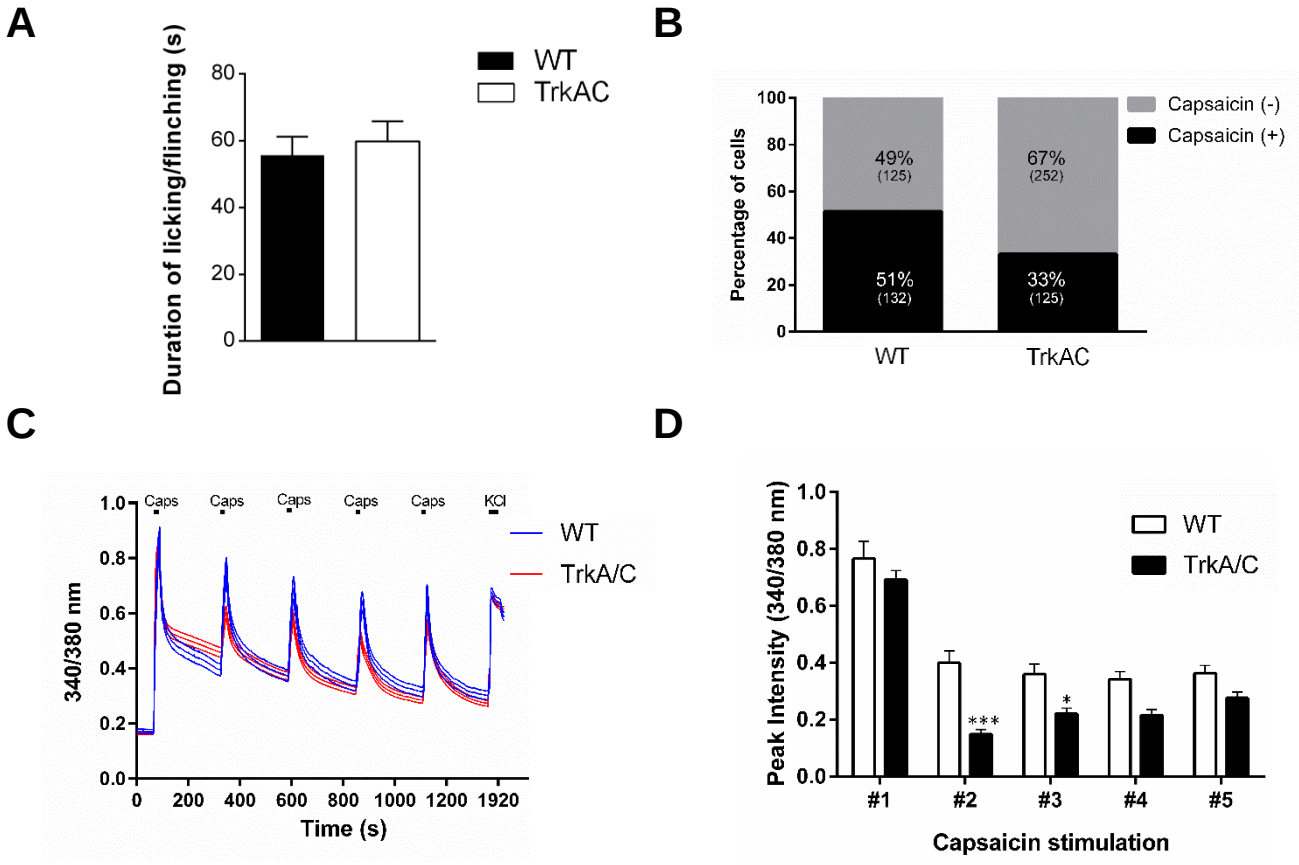
A
Duration of licking/flinching (s)
80
60
40
20
0
WT
TrkAC
B
Percentage of cells
100
80
60
40
20
0
49%
(125)
51%
(132)
67%
(252)
33%
(125)
Capsaicin (-)
Capsaicin (+)
WT
TrkAC
C
Caps
Caps
Caps
Caps
Caps
KCl
1.0
0.8
0.6
0.4
0.2
0.0
340/380 nm
0
200
400
600
800
1000
1200
1920
Time (s)
WT
TrkA/C
D
Peak Intensity (340/380 nm)
1.0
0.8
0.6
0.4
0.2
0.0
***
*
#1
#2
#3
#4
#5
Capsaicin stimulation
WT
TrkA/C

Figure 3

Figure 4

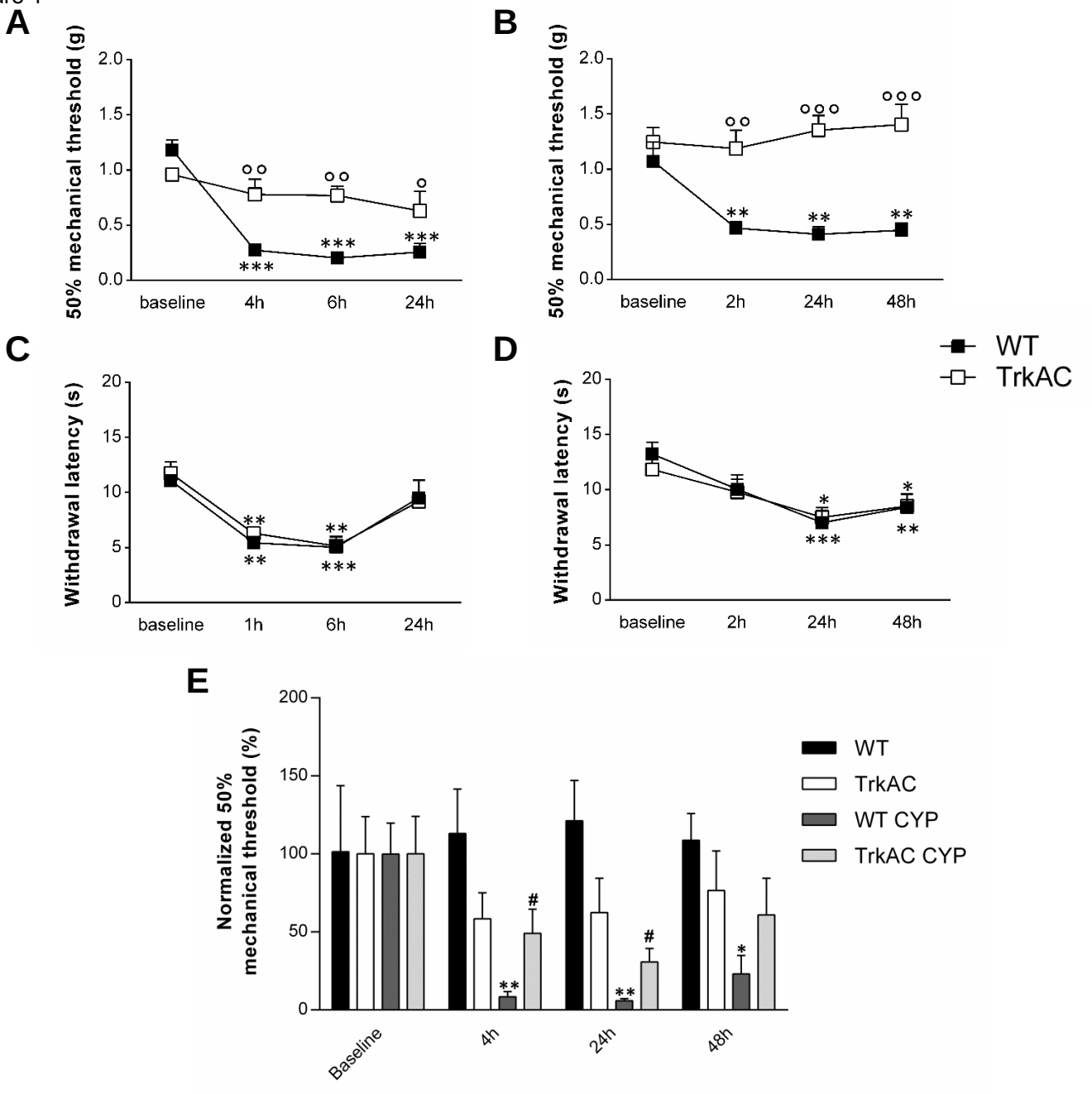

Figure 1

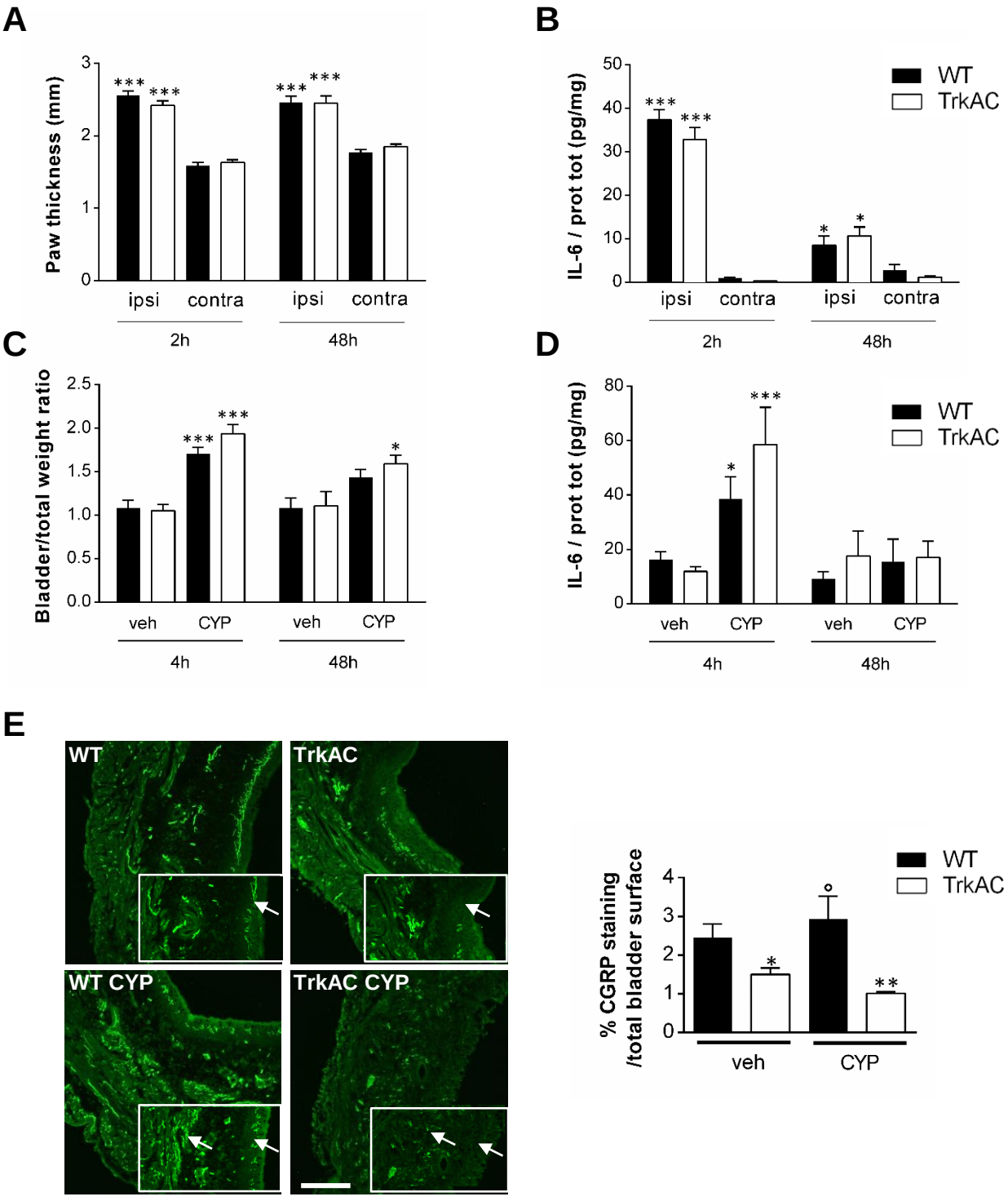
A
Paw thickness (mm)
ipsi
contra
ipsi
contra
2h
48h
B
IL-6 / prot tot (pg/mg)
WT
TrkAC
ipsi
contra
ipsi
contra
2h
48h
C
Bladder/total weight ratio
veh
CYP
veh
CYP
4h
48h
D
IL-6 / prot tot (pg/mg)
WT
TrkAC
veh
CYP
veh
CYP
4h
48h
E
WT
TrkAC
WT CYP
TrkAC CYP
% CGRP staining /total bladder surface
WT
TrkAC
veh
CYP

Figure 2

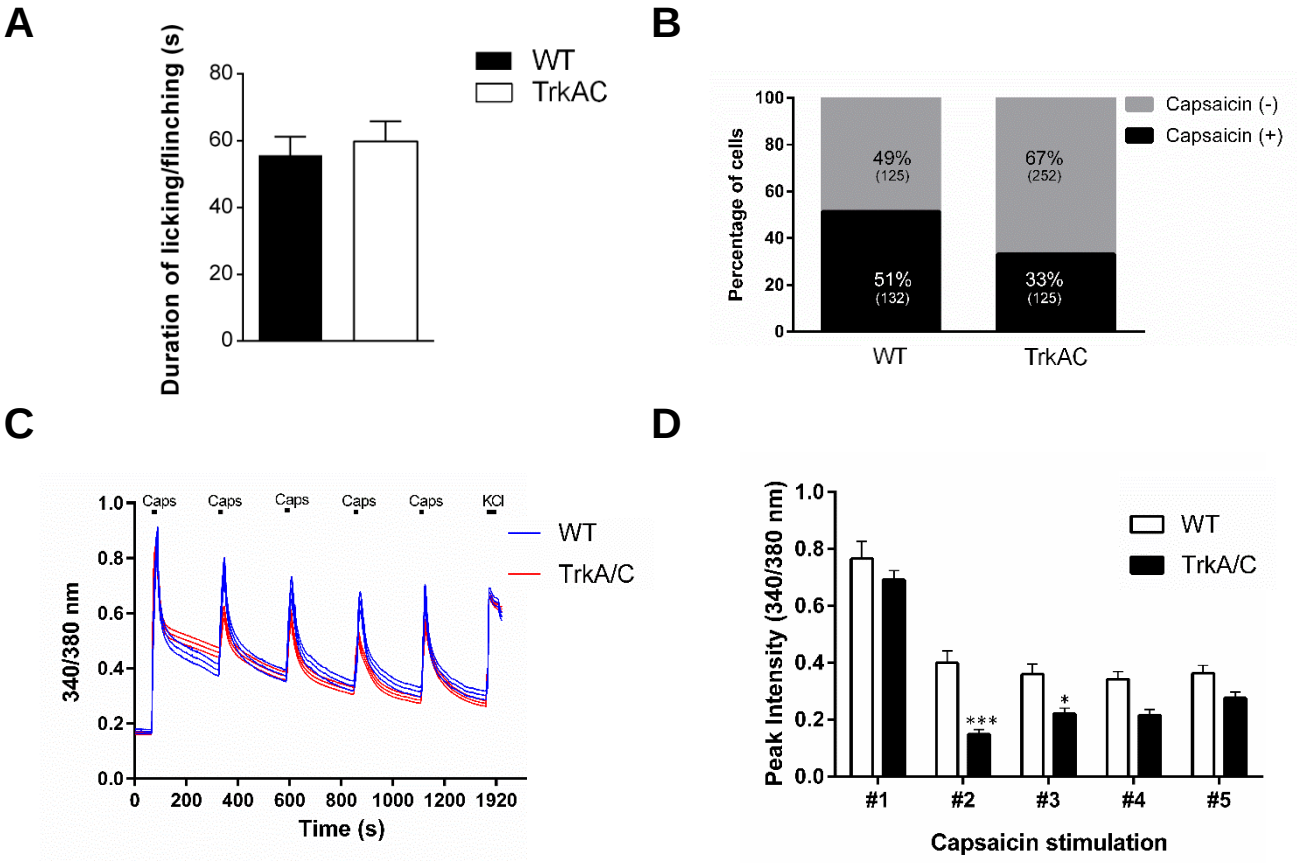
A
Duration of licking/flinching (s)
80
60
40
20
0
WT
TrkAC
B
Percentage of cells
100
80
60
40
20
0
49%
(125)
51%
(132)
67%
(252)
33%
(125)
Capsaicin (-)
Capsaicin (+)
WT
TrkAC
C
340/380 nm
1.0
0.8
0.6
0.4
0.2
0.0
Caps
Caps
Caps
Caps
Caps
KCl
0
200
400
600
800
1000
1200
1920
Time (s)
WT
TrkA/C
D
Peak Intensity (340/380 nm)
1.0
0.8
0.6
0.4
0.2
0.0
***
*
#1
#2
#3
#4
#5
Capsaicin stimulation
WT
TrkA/C

Figure 3

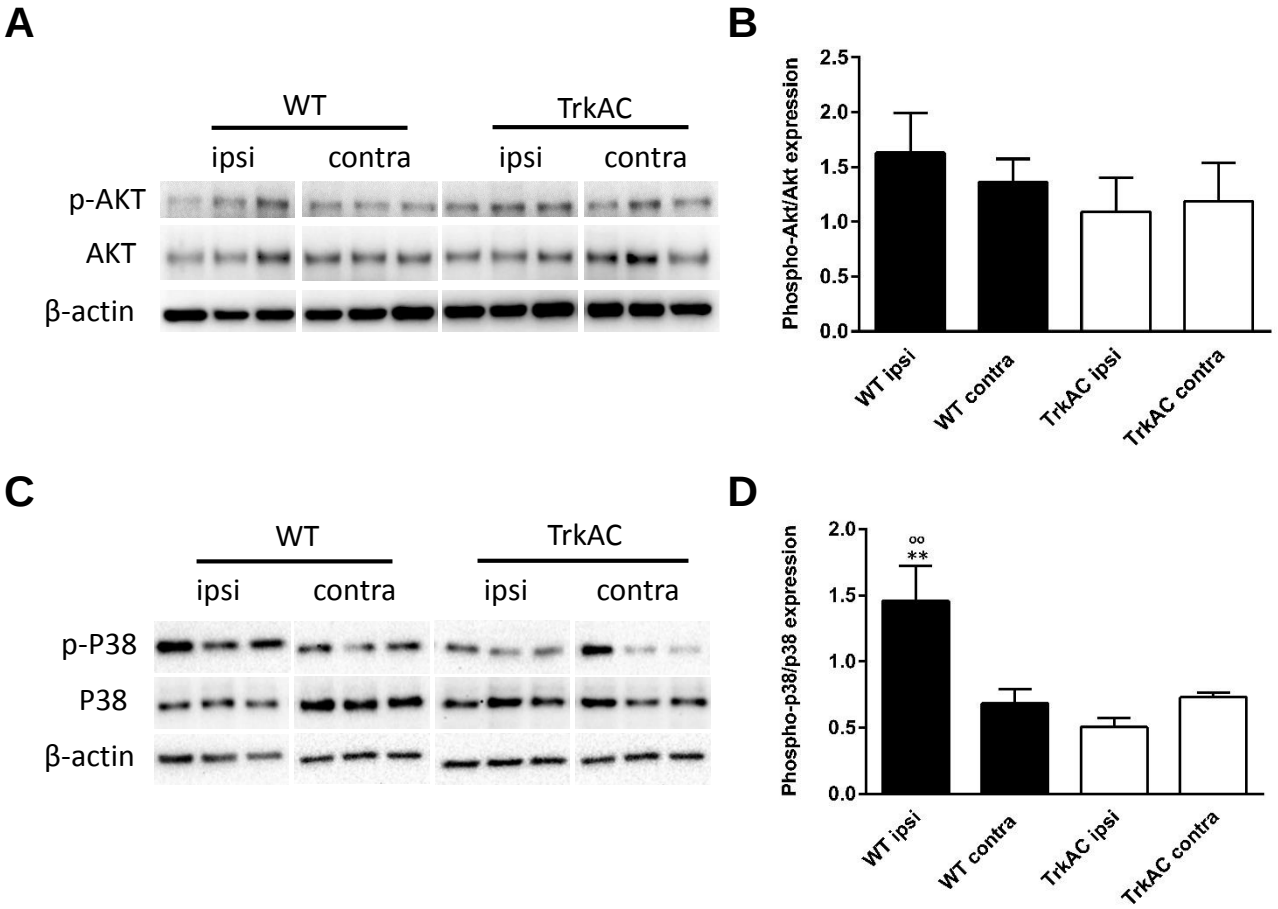
A
WT
TrkAC
ipsi
contra
ipsi
contra
p-AKT
AKT
β-actin
B
Phospho-Akt/Akt expression
2.5
2.0
1.5
1.0
0.5
0.0
WT ipsi
WT contra
TrkAC ipsi
TrkAC contra
C
WT
TrkAC
ipsi
contra
ipsi
contra
p-P38
P38
β-actin
D
Phospho-p38/p38 expression
2.0
1.5
1.0
0.5
0.0
°°
**
WT ipsi
WT contra
TrkAC ipsi
TrkAC contra

Figure 4

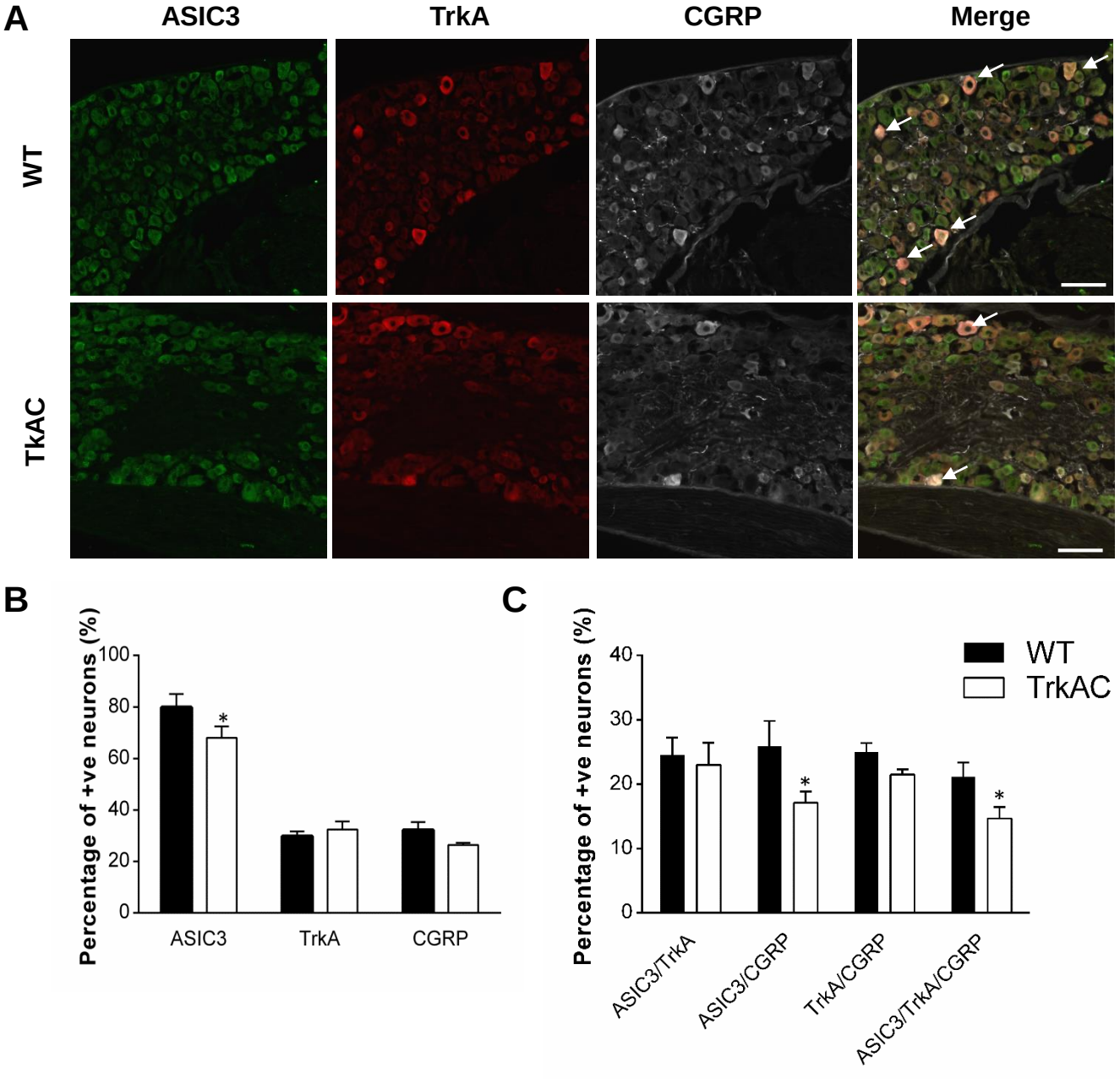
A
ASIC3
TrkA
CGRP
Merge
WT
TkAC
B
Percentage of +ve neurons (%)
100
80
60
40
20
0
*
ASIC3
TrkA
CGRP
C
Percentage of +ve neurons (%)
40
30
20
10
0
WT
TrkAC
*
*
ASIC3/TrkA
ASIC3/CGRP
TrkA/CGRP
ASIC3/TrkA/CGRP

Figure 5

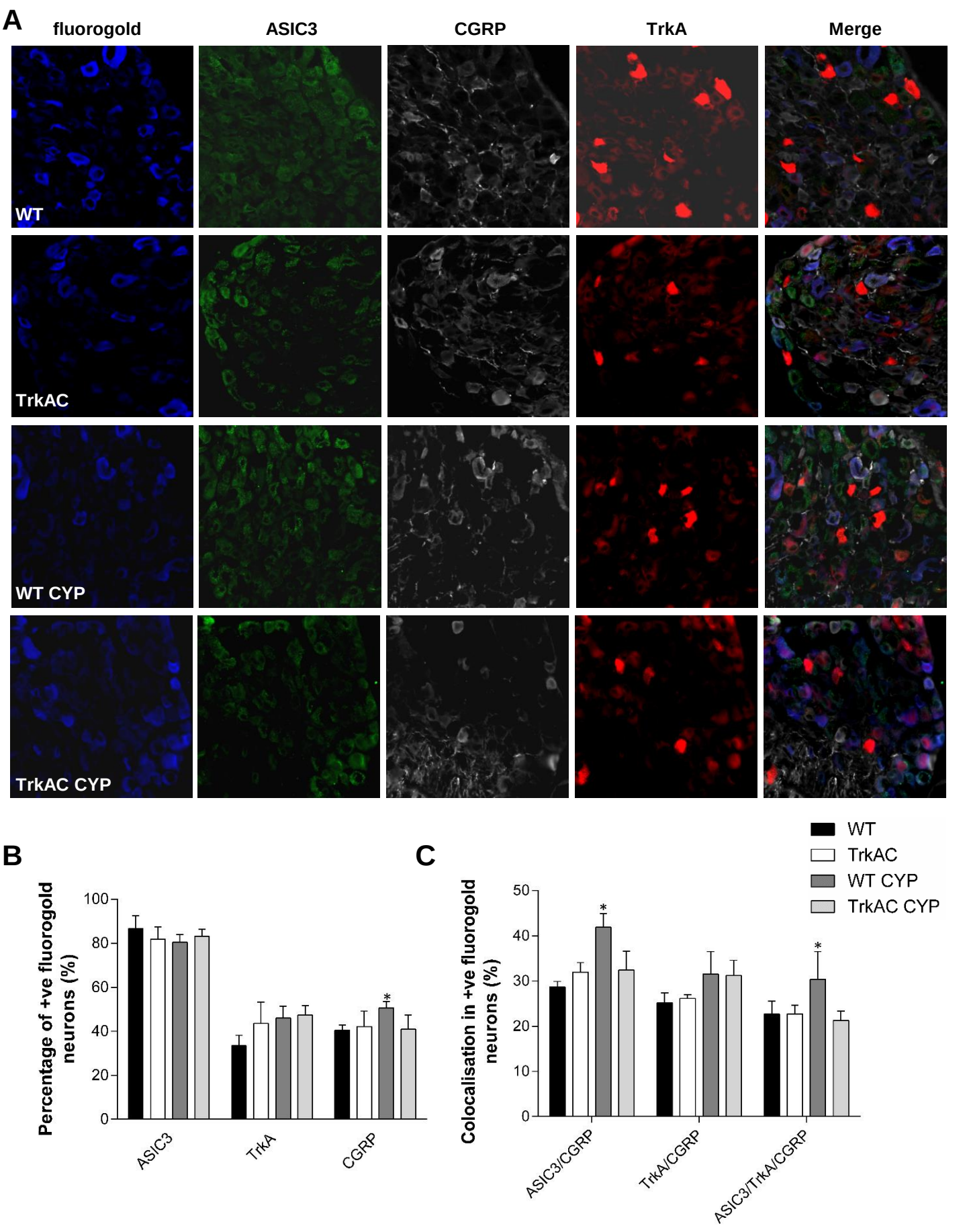
A
fluorogold
ASIC3
CGRP
TrkA
Merge
WT
TrkAC
WT CYP
TrkAC CYP
B
Percentage of +ve fluorogold neurons (%)
100
80
60
40
20
0
ASIC3
TrkA
CGRP
*
C
Colocalisation in +ve fluorogold neurons (%)
50
40
30
20
10
0
ASIC3/CGRP
TrkA/CGRP
ASIC3/TrkA/CGRP
*
*
WT
TrkAC
WT CYP
TrkAC CYP

Figure 6

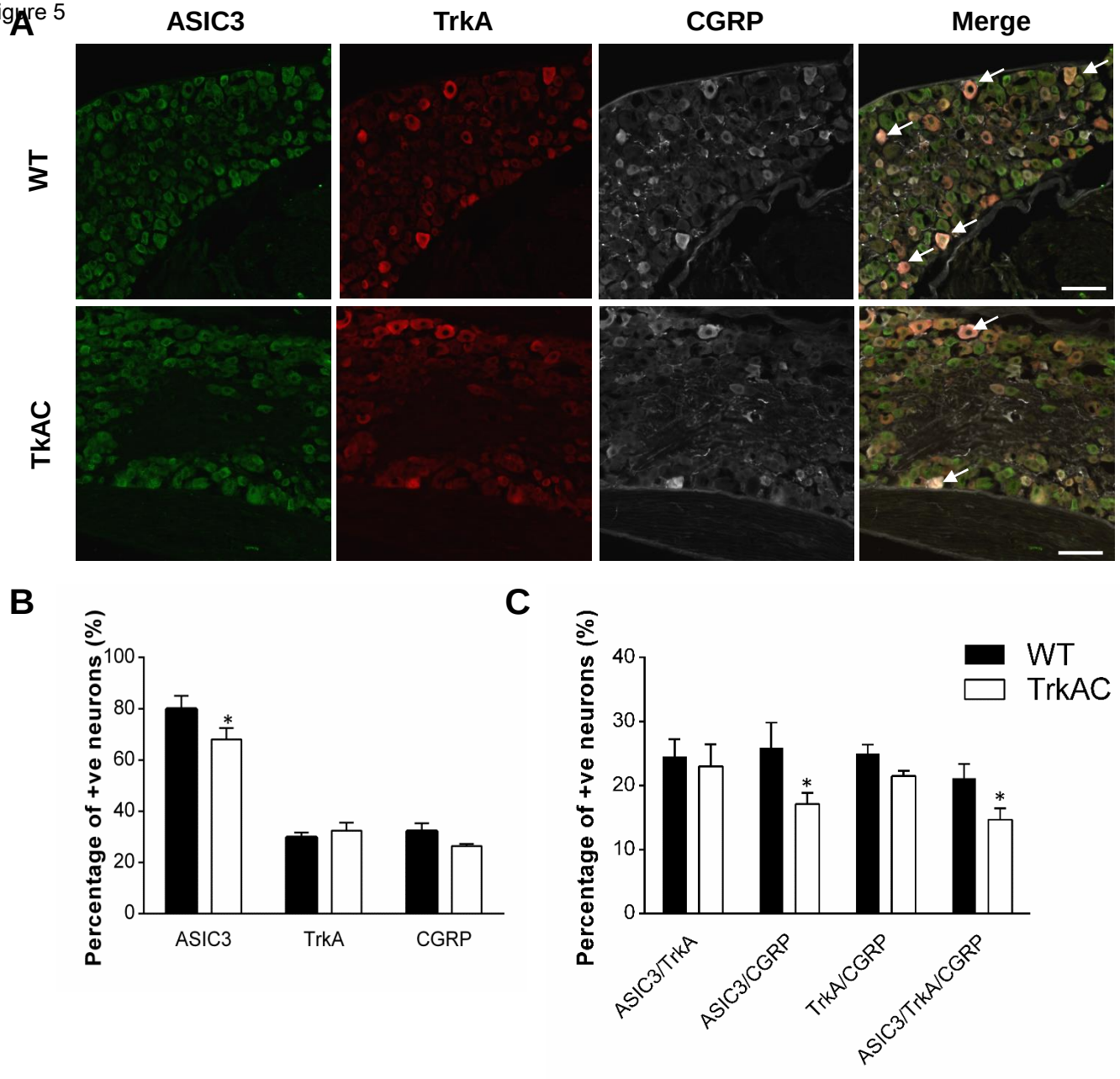
A
ASIC3
TrkA
CGRP
Merge
WT
TkAC
B
Percentage of +ve neurons (%)
100
80
60
40
20
0
*
ASIC3
TrkA
CGRP
C
Percentage of +ve neurons (%)
40
30
20
10
0
WT
TrkAC
*
*
ASIC3/TrkA
ASIC3/CGRP
TrkA/CGRP
ASIC3/TrkA/CGRP

Figure 5

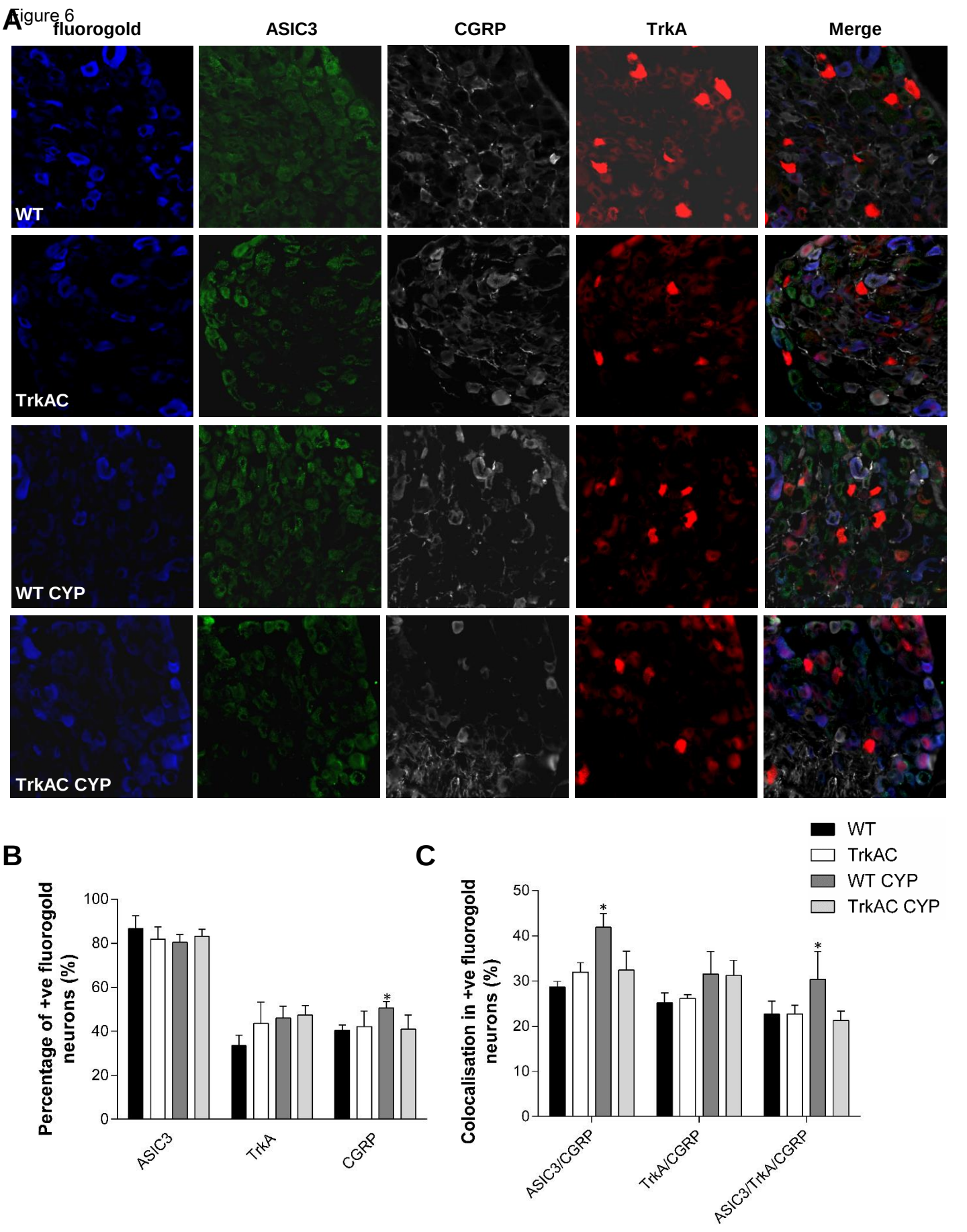
A
fluorogold
ASIC3
CGRP
TrkA
Merge
WT
TrkAC
WT CYP
TrkAC CYP
B
Percentage of +ve fluorogold neurons (%)
100
80
60
40
20
0
ASIC3
TrkA
CGRP
*
C
Colocalisation in +ve fluorogold neurons (%)
50
40
30
20
10
0
ASIC3/CGRP
TrkA/CGRP
ASIC3/TrkA/CGRP
*
*
WT
TrkAC
WT CYP
TrkAC CYP

Figure 6

Table 1

Gene	Primer sequences (5'->3')
AKT1	F : GACGTAGCCATTGTGAAGGA (20) R : CATCGTTCTTGAGGAGGAAGTAG (23)
ASIC3	F : CACCCAATGACTTGCACTGG (20) R : TAGGCAGCATGTTCAGCAGG (20)
MAPK14	F : CTATGGCTCGGTGTGTGCT (19) R : GACGCAACTCTCGGTAGGTC (20)
MAPK3	F : AATTGGTCAGGACAAGGGCT (20) R : GAGTGGGTAAGCTGAGACGG (20)
MAPK1	F : TCCATTCAGCTAACGTTCTGC (21) R : GTACTCTGTCAAGAACCCTGTG (22)
PRKCZ	F : GGCTGCAAGACTTCGACCTCATC (23) R : CTGGACGCCTGCTCAAACACATGT(24)
JUN	F : CTCCGGACTGTTCATCCGTT (20) R : GGGACTCTCCAAATGCTCCC (20)
PRKACA	F : GTCATGGAGTATGTAGCTGGTG (22) R : CAGATACTCAAAGGTCAGGACG (22)
PRKCA	F : GAAGGGCACATCAAAATCGC (20) R : CACCAATCTACAGACTTCCCG (21)

Table 2

Antibodies	Dilution	Manufacturer
Guinea pig anti-ASIC3	1/200	#AB5927, Merck Millipore (France)
Rabbit anti-TrkA	1/2000	Generous gift from Dr Reichardt
Mouse anti-CGRP	1/1000	#S57053, Santa Cruz (USA)
Rabbit anti-CGRP	1/1000	#PC205, Calbiochem (France)
Rabbit anti PGP 9.5	1/400	#E3340, Spring Bioscience (USA)
Goat anti guinea pig-488	1/1000	Alexa fluor (Molecular Probes, USA)
Goat anti rabbit-546	1/1000	Alexa fluor (Molecular Probes, USA)
Donkey anti mouse-647	1/1000	Alexa fluor (Molecular Probes, USA)

Table 3

Incision	WT ipsi	WT contra	TrkAC ipsi	TrkAC contra
Akt1	2.83 ± 0.19*****	1.06 ± 0.19	0.69 ± 0.12	0.51 ± 0.04
Mapk14 (P38)	3.35 ± 0.08*****	1.05 ± 0.16	0.95 ± 0.14	0.93 ± 0.05
Mapk3 (Erk1)	2.69 ± 0.77	1.07 ± 0.2	0.97 ± 0.12	0.97 ± 0.09
Mapk1 (Erk2)	1.07 ± 0.06	1.15 ± 0.29	1.22 ± 0.08	0.95 ± 0.08
Jun	8.74 ± 1.04*****	1.49 ± 0.74	1.94 ± 0.33	1.47 ± 0.10
Prkca (Pkc)	0.93 ± 0.01	1.01 ± 0.10	1.08 ± 0.10	0.97 ± 0.06
Prkcz (Pkmz)	1.05 ± 0.05	1.09 ± 0.07	1.10 ± 0.09	1.10 ± 0.11
Prkaca (Pka)	1.04 ± 0.31	1.41 ± 0.32	1.42 ± 0.25	1.88 ± 0.21
Accn3	0.67 ± 0.07*****	1.01 ± 0.06	0.47 ± 0.02***°**	0.76 ± 0.06
Cystitis	WT	WT CYP	TrkAC	TrkAC CYP
Akt1	1.08 ± 0.17	0.69 ± 0.12	0.88 ± 0.05	0.81 ± 0.10
Mapk14 (P38)	1.04 ± 0.15	0.63 ± 0.1	0.78 ± 0.05	0.73 ± 0.11
Jun	1.37 ± 0.38	0.60 ± 0.10	0.74 ± 0.04	0.90 ± 0.34
Accn3	1.01 ± 0.1	0.89 ± 0.13	0.55 ± 0.07	0.58 ± 0.16

A

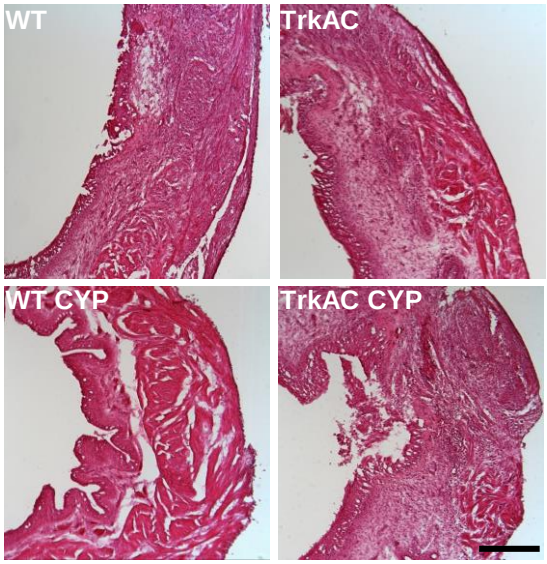

B

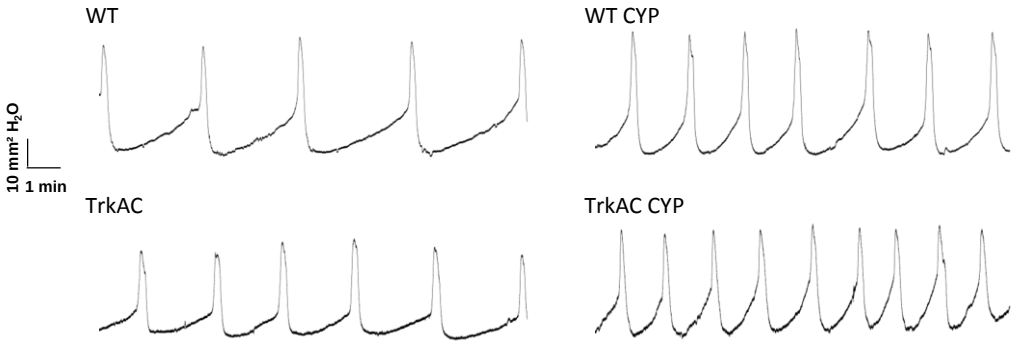

C

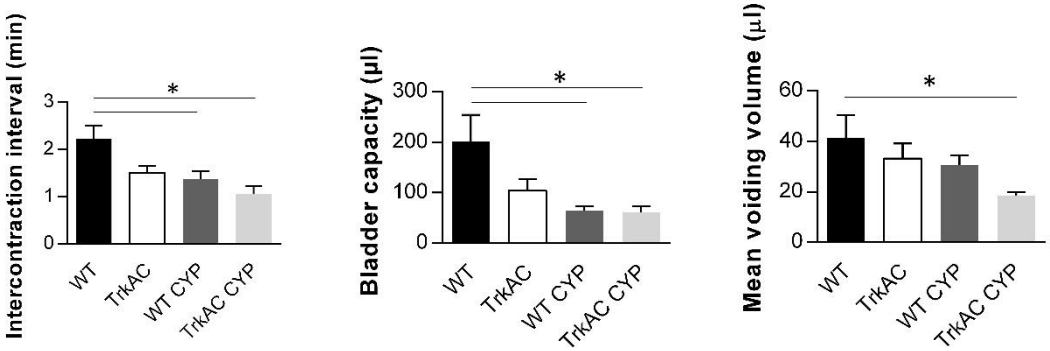

D

	WT	TrkAC	WT CYP	TrkAC CYP
Maximum bladder pressure (cmH_2O)	42.7 ± 2.4	40.4 ± 8.3	43.7 ± 6.3	35.5 ± 3.9
Contraction threshold (cmH_2O)	24.2 ± 1.5	22.5 ± 5.8	19.0 ± 3.4	20.2 ± 2.0
Resting pressure (cmH_2O)	16.4 ± 1.8	15.5 ± 4.8	12.7 ± 3.8	14.9 ± 2.1
Contraction amplitude (cmH_2O)	18.6 ± 1.3	17.9 ± 2.6	24.7 ± 2.8	15.3 ± 2.3

Supplementary Figure 1

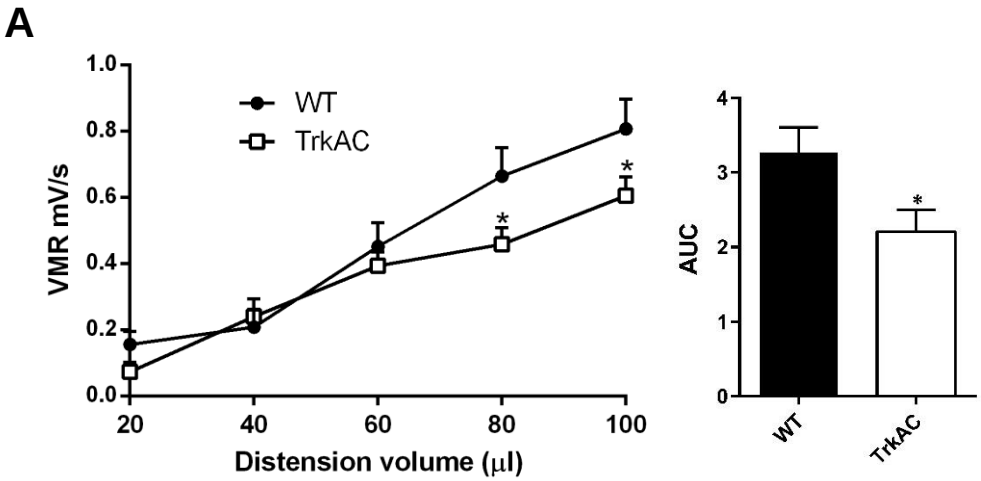

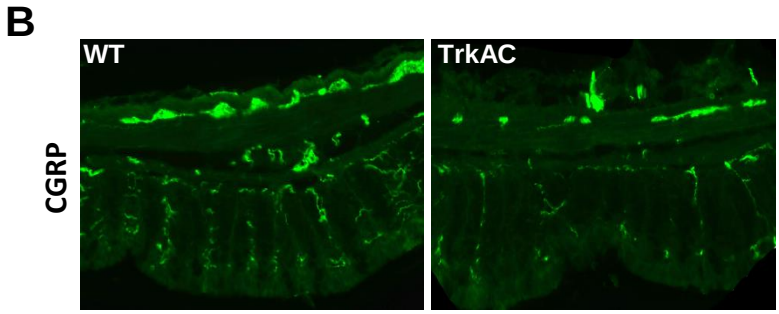

Supplementary Figure 2

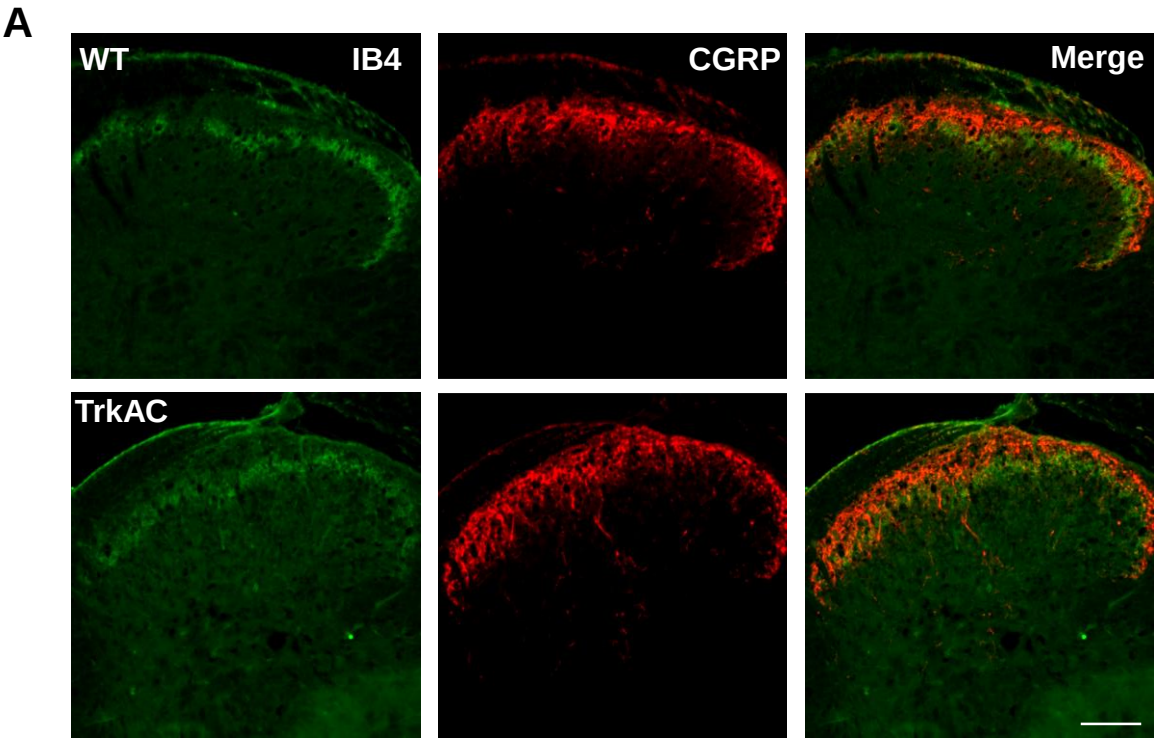

Supplementary Figure 3

Supplementary methods

Supplementary Figure 1

Bladder histology

In **supplementary Fig.1A**, bladder sections from each group (CYP or saline) and genotype (WT or TrkAC), were stained with Hematoxilin/Eosin for histology. Representative photomicrographs of bladder sections were taken using a Zeiss Scope A1 microscope running Axiovision 4.8 image analysis software.

Cystometry

In **supplementary Fig.1B**, forty eight hours after CYP or saline administration in WT and TrkAC mice, animals were anesthetized with a mixture of xylazine hydrochloride (Rompun®, 0.4 mg/kg) and ketamine (Imalgene 500®, 100 mg/kg) and placed in a supine position. Abdominal skin was shaved, cleaned with povidone iodine 10% (Merck) and the abdomen carefully opened to expose the bladder. A PE10 catheter with a collar was then inserted through the apex of the bladder and secured with 5.0 sutures (Ethicon, Somerville, NJ, USA). The bladder was then emptied. Perfusion of NaCl 0.9% was realized at the rate of 20µL/min. After bladder instillation started, the system was allowed to stabilize to achieve a stable contraction/voiding pattern prior to data collection for analysis. Recording of intra-bladder pressure was then realized for at least 1h with a pressure transducer (Harvard Apparatus, USA) connected to a catheter with a three way tap with the fluid filled pressure at one end, and injection pumps (Harvard Apparatus, USA) to the other. The pressure transducer was connected to a preamp (Harvard Apparatus, USA), amplified (Power-Lab®, AD Instruments, Oxford, UK) and recorded on a computer running Labchart® (AD

Instrument, Oxford, UK). Voided volume was collected on a pre-weighted cotton swab for each voiding contraction (**supplementary Fig.1C,** right histogram). Analysis of the pressure recording allow to measure inter contraction interval, maximum contraction amplitude, resting pressure, threshold pressure and maximum bladder pressure (**supplementary Fig. 1C&D**), as previously described (Andersson, Soler and Füllhase, 2011). n=5-6 for each group and genotype (WT + saline, TrkAC + saline, WT + CYP and TrkAC + CYP).

Supplementary Figure 2

Assessment of colonic sensitivity using colorectal distension

In **supplementary Fig. 2A**, mice colonic sensitivity in 10-12 weeks old naive WT and TrkAC mice was assessed by quantifying visceromotor response (VMR) with abdominal electromyogram recordings in response to colorectal distension (CRD) (Christianson and Gebhart, 2007). Prior to colonic sensitivity measurement, mice were anaesthetized with an intraperitoneal injection with a mixture of xylazine hydrochloride (Rompun®, 0.4 mg/kg) and ketamine (Imalgene 500®,100 mg/kg), the left abdominal external musculature was exposed by skin incision and two nickel-chromium electrodes (Nikrothal 80, Kanthal, Sweden) were implanted into the abdominal oblique muscle. Electrodes were secured with 5-0 sutures (Ethicon, Somerville, NJ, USA). Skin wound was then closed with 3-0 sutures. The opposite electrode ends were externalized subcutaneously through an incision at the back of the neck and wrapped around a polyethylene catheter attached to the skin with three 3-0 sutures (Ethicon, Somerville, NJ, USA). Mice were allowed to recover for at least five days before experiments.

On the experimental day, mice were acclimatised to the restraint device for 2h before colorectal distension. They were then briefly anaesthetized (1.5% Isoflurane) to insert the distension probe (Fogarty Arterial Embolectomy Catheter 4, Edward Life science, CA, USA) at 1cm from the anal margin, and a nickel-chromium reference electrode (Nikrothal 80, Kanthal, Sweden) was inserted subcutaneously within the tail. Animals were replaced in the restriction cages and allowed to recover for 30 min prior to colorectal distension. Electrodes were connected to a Bio-Amp® recording system (AD Instruments, Oxford, UK) linked to an acquisition interface device (Power-Lab®, AD Instruments, Oxford, UK). Electromyographic signal was amplified, filtered at 100Hz, integrated and smoothed. Colorectal distension was performed by inflating the distension probe from 20µL to 100µL, by 20µL incremental step. A 5min interval period was observed between each stimulation. Recording was performed 10s before stimulation (baseline) and 10s during the stimulation period. Visceromotor responses were quantified as the area under the electromyogram activity curve during the 10s stimulation period minus the area measured during the 10s baseline. n=8 for each genotype (*i.e.* 8 WT and 8 TrkAC).

Following colorectal distension, 4 WT and 4 TrkAC mice were terminally anaesthetised using pentobarbitone and quickly perfused transcardially with NaCl 0.9% followed by 4% PFA. Colon were excised, post-fixed for 12h in the same perfusion fixative, cryoprotected in 30% sucrose in 0.1 M phosphate buffer (PB) for 48h at 4°C, and then frozen in OCT. Transverse sections (20µm) were cut on cryostat, dried for 30 min at room temperature and then stored at -20°C before staining. Colon sections were stained with the primary antibody against CGRP (rabbit anti-CGRP, 1:1000, Calbiochem) diluted in the antibody diluent (#S2022; Dako). Following 5 washes of 5 min in PBS, sections were incubated with the appropriate secondary

antibody (goat anti-rabbit, 1/1000, Alexa fluor 488) diluted in the same antibody diluent for 2h at room temperature. Sections were then washed 3 times in PBS and cover-slipped with fluorescent mounting medium (Dako). Colon sections were visualised under a Nikon Eclipse Ni-E fluorescent microscope run with Nikon analysis software (NiS element). Representative photomicrograph are presented in **supplementary Fig. 2B**.

Following colorectal distension, the remaining 4 WT and 4 TrkAC mice were also terminally anaesthetised using pentobarbitone and caecum, colon and spleen were freshly dissected out and weighted. Total length of the colon was also measured. There was no significant difference between WT and TrkAC mice in these different anatomical parameters (data not shown).

Supplementary Figure 3

Assessment of TrkA trafficking

To assess if NGF/TrkA complex trafficking from the periphery toward the DRG cell bodies was not affected in TrkAC mice, at the same time at the left hind paw incision was made, we carefully exposed the left sciatic nerve and tightly ligated the nerve with one 5.0 suture in 2 WT and 2 TrkAC mice. 48h after the surgery, mice were terminally anaesthetised using pentobarbitone and quickly perfused transcardially with NaCl 0.9% followed by 4% PFA. After perfusion, the left sciatic nerve were excised, post-fixed for 4h in the same perfusion fixative, cryoprotected in 30% sucrose in 0.1 M phosphate buffer (PB) for 48h at 4°C, and then frozen in tissue freezing medium (O.C.T.). Longitudinal sections (20µm) of the left sciatic nerve were cut on cryostat, dried for 30 min at room temperature and then stored at -20°C before staining. Sciatic nerve sections were stained with the primary antibody against TrkA (rabbit anti-TrkA,

1:2000, generous gift from Dr Reichardt) and the appropriate secondary antibody (1:1000, goat anti-rabbit Alexa fluor 546) as described for DRG sections. Sciatic nerve sections were visualised under a Nikon Eclipse Ni-E fluorescent microscope run with Nikon analysis software (NiS element) and representative photomicrographs were taken and presented in **supplementary Fig. 3A**.

Spinal cord immunohistochemistry

Two animals of each genotype (*i.e.* WT and TrkAC) were terminally anaesthetised using pentobarbitone and quickly perfused transcardially with saline followed by 4% paraformaldehyde (PFA). After perfusion, lumbar spinal cord were excised, post-fixed 12h in the same perfusion fixative, cryoprotected in 30% sucrose in 0.1 M phosphate buffer (PB) for at least 48h at 4°C, and then frozen in tissue freezing medium (O.C.T). Transverse spinal cord sections (20µm) were cut on cryostat, dried for 30 min at room temperature and then stored at -20°C before staining.

Spinal cord sections were stained as follow: after 3 washes in PBS containing 0.2% triton X-100 and 1% BSA, sections were incubated overnight at room temperature in a humid chamber with the following primaries antibodies: rabbit anti-CGRP (1/1000, Calbiochem) and Isolectin B4-FITC (1/1000, L2895, Sigma-Aldrich) in antibody diluent (#S2022; Dako). Following 5 washes 5 min each in PBS, sections were then incubated with the secondary antibody for CGRP (1:1000, goat anti rabbit Alexa fluor 546) diluted in the same antibody diluent for 2h at room temperature. Sections were then washed 3 times in PBS and cover-slipped with fluorescent mounting medium (Dako). Sections were visualised under a Nikon Eclipse Ni-E fluorescent microscope run with Nikon analysis software (NiS element) and representative pictures were taken and presented in **supplementary Fig. 3B**.

Please wait...

If this message is not eventually replaced by the proper contents of the document, your PDF viewer may not be able to display this type of document.

You can upgrade to the latest version of Adobe Reader for Windows®, Mac, or Linux® by visiting http://www.adobe.com/go/reader_download.

For more assistance with Adobe Reader visit http://www.adobe.com/go/acrreader.

Please wait...

If this message is not eventually replaced by the proper contents of the document, your PDF viewer may not be able to display this type of document.

You can upgrade to the latest version of Adobe Reader for Windows®, Mac, or Linux® by visiting http://www.adobe.com/go/reader_download.

For more assistance with Adobe Reader visit http://www.adobe.com/go/acrreader.

Please wait...

If this message is not eventually replaced by the proper contents of the document, your PDF viewer may not be able to display this type of document.

You can upgrade to the latest version of Adobe Reader for Windows®, Mac, or Linux® by visiting http://www.adobe.com/go/reader_download.

For more assistance with Adobe Reader visit http://www.adobe.com/go/acrreader.

Please wait...

If this message is not eventually replaced by the proper contents of the document, your PDF viewer may not be able to display this type of document.

You can upgrade to the latest version of Adobe Reader for Windows®, Mac, or Linux® by visiting http://www.adobe.com/go/reader_download.

For more assistance with Adobe Reader visit http://www.adobe.com/go/acrreader.

Please wait...

If this message is not eventually replaced by the proper contents of the document, your PDF viewer may not be able to display this type of document.

You can upgrade to the latest version of Adobe Reader for Windows®, Mac, or Linux® by visiting http://www.adobe.com/go/reader_download.

For more assistance with Adobe Reader visit http://www.adobe.com/go/acrreader.

Please wait...

If this message is not eventually replaced by the proper contents of the document, your PDF viewer may not be able to display this type of document.

You can upgrade to the latest version of Adobe Reader for Windows®, Mac, or Linux® by visiting http://www.adobe.com/go/reader_download.

For more assistance with Adobe Reader visit http://www.adobe.com/go/acrreader.

Please wait...

If this message is not eventually replaced by the proper contents of the document, your PDF viewer may not be able to display this type of document.

You can upgrade to the latest version of Adobe Reader for Windows®, Mac, or Linux® by visiting http://www.adobe.com/go/reader_download.

For more assistance with Adobe Reader visit http://www.adobe.com/go/acrreader.

Please wait...

If this message is not eventually replaced by the proper contents of the document, your PDF viewer may not be able to display this type of document.

You can upgrade to the latest version of Adobe Reader for Windows®, Mac, or Linux® by visiting http://www.adobe.com/go/reader_download.

For more assistance with Adobe Reader visit http://www.adobe.com/go/acrreader.

Please wait...

If this message is not eventually replaced by the proper contents of the document, your PDF viewer may not be able to display this type of document.

You can upgrade to the latest version of Adobe Reader for Windows®, Mac, or Linux® by visiting http://www.adobe.com/go/reader_download.

For more assistance with Adobe Reader visit http://www.adobe.com/go/acrreader.

Please wait...

If this message is not eventually replaced by the proper contents of the document, your PDF viewer may not be able to display this type of document.

You can upgrade to the latest version of Adobe Reader for Windows®, Mac, or Linux® by visiting http://www.adobe.com/go/reader_download.

For more assistance with Adobe Reader visit http://www.adobe.com/go/acrreader.

Please wait...

If this message is not eventually replaced by the proper contents of the document, your PDF viewer may not be able to display this type of document.

You can upgrade to the latest version of Adobe Reader for Windows®, Mac, or Linux® by visiting http://www.adobe.com/go/reader_download.

For more assistance with Adobe Reader visit http://www.adobe.com/go/acrreader.

Please wait...

If this message is not eventually replaced by the proper contents of the document, your PDF viewer may not be able to display this type of document.

You can upgrade to the latest version of Adobe Reader for Windows®, Mac, or Linux® by visiting http://www.adobe.com/go/reader_download.

For more assistance with Adobe Reader visit http://www.adobe.com/go/acrreader.

Please wait...

If this message is not eventually replaced by the proper contents of the document, your PDF viewer may not be able to display this type of document.

You can upgrade to the latest version of Adobe Reader for Windows®, Mac, or Linux® by visiting http://www.adobe.com/go/reader_download.

For more assistance with Adobe Reader visit http://www.adobe.com/go/acrreader.

Please wait...

If this message is not eventually replaced by the proper contents of the document, your PDF viewer may not be able to display this type of document.

You can upgrade to the latest version of Adobe Reader for Windows®, Mac, or Linux® by visiting http://www.adobe.com/go/reader_download.

For more assistance with Adobe Reader visit http://www.adobe.com/go/acrreader.